Satellite-based mapping of canopy fuels at the pan-European scale

Erico Kutchartt, José Ramón González-Olabarria, Antoni Trasobares, Núria
Aquilué, Juan Guerra-Hernández, Leónia Nunes, Ana Catarina Sequeira,
Brigite Botequim, Marius Hauglin, Palaiologos Palaiologou, et al.

HAL Id: hal-04904648

https://hal.inrae.fr/hal-04904648v1

Submitted on 21 Jan 2025

Satellite-based mapping of canopy fuels at the pan-European scale

Erico Kutchartt, José Ramón González-Olabarria, Antoni Trasobares, Núria Aquilué, Juan Guerra-Hernández, Leónia Nunes, Ana Catarina Sequeira, Brigite Botequim, Marius Hauglin, Palaiologos Palaiologou, Adrian Cardil, Martino Rogai, Vassil Vassilev, Francois Pimont, Olivier Martin-Ducup & Francesco Pirotti

Taylor & Francis
Taylor & Francis Group

Satellite-based mapping of canopy fuels at the pan-European scale

Erico Kutchartt [a,b], José Ramón González-Olabarria [a,c], Antoni Trasobares [a], Núria Aquilué [a,c], Juan Guerra-Hernández [d], Leónia Nunes [e], Ana Catarina Sequeira [e], Brigite Botequim [f], Marius Hauglin [g], Palaiologos Palaiologou [h], Adrian Cardil [a,i], Martino Rogai [j], Vassil Vassilev [k], Francois Pimont [l], Olivier Martin-Ducup [l] and Francesco Pirotti [b,m]

[a]Forest Science and Technology Centre of Catalonia (CTFC), Carretera de Sant Llorenç de Morunys, Solsona, Spain; [b]Department of Land, Environment, Agriculture and Forestry (TESAF), University of Padova, Legnaro (PD), Italy; [c]Joint Research Unit CTFC - AGROTECNIO, Carretera de Sant Llorenç de Morunys, Solsona, Spain; [d]Forest Research Centre, Associate Laboratory TERRA, School of Agriculture (ISA), University of Lisbon, Lisbon, Portugal; [e]Centre for Applied Ecology "Professor Baeta Neves" (CEABN), InBIO, School of Agriculture (ISA), University of Lisbon, Lisbon, Portugal; [f]ForestWISE - Collaborative Laboratory for Integrated Forest & Fire Management, Quinta de Prados, Vila Real, Portugal; [g]Division of Forestry and Forest Resources, Norwegian Institute of Bioeconomy Research (NIBIO), As, Norway; [h]Department of Forestry and Natural Environment Management, Agricultural University of Athens (AUA), Karpenisi, Greece; [i]Technosylva, Parque Tecnológico de León, León, Spain; [j]Consiglio Nazionale delle Ricerche (CNR), Istituto per la BioEconomia, Sesto Fiorentino (FI), Italy; [k]Space Research and Technology Institute, Bulgarian Academy of Sciences, Sofia, Bulgaria; [l]Ecologie des Forêts Méditerranéennes (URFM), INRAE, Avignon, France; [m]Interdepartmental Research Center of Geomatics (CIRGEO), University of Padova, Legnaro (PD), Italy

ABSTRACT
Canopy base height (CBH) and canopy bulk density (CBD) are forest canopy fuel parameters that are key for modeling the behavior of crown wildfires. In this work, we map them at a pan-European scale for the year 2020, producing a new dataset consisting of two raster layers containing both variables at an approximate resolution of 100 m. Spatial data from Earth observation missions and derived down-stream products were retrieved and processed using artificial intelligence to first estimate a map of aboveground biomass (AGB). Allometric models were then used to estimate the spatial distribution of CBH using the canopy height values as explanatory variables and CBD using AGB values. Ad-hoc allometric models were defined for this study. Data provided by FIRE-RES project partners and acquired through field inventories was used for validating the final products using an independent dataset of 804 ground-truth sample plots. The CBH and CBD raster maps have, respectively, the following accuracy regarding specific metrics reported from the modeling procedures: (i) coefficient of correlation (R) of 0.445 and 0.330 (p-value < 0.001); (ii) root mean square of error (RMSE) of 3.9 m and 0.099 kg m^{-3}; and (iii) a mean absolute percentage error (MAPE) of 61% and 76%. Regarding CBD, the accuracy metrics improved in closed canopies (canopy cover > 80%) to $R = 0.457$, RMSE = 0.085, and MAPE = 59%. In short, we believe that the degree of accuracy is reasonable in the resulting maps, producing CBH and CBD datasets at the pan-European scale to support fire mitigation and crown fire simulations.

1. Introduction

There are more than two million wildfire events recorded every year worldwide, causing substantial economic, social, and environmental impacts (Bowman et al. 2017; Kalogiannidis et al. 2023; Tedim et al. 2018). In Europe, around 8,000 fires have occurred during 2022, which have affected 837,212 ha, including only the countries as part of the EU-27 (San-Miguel-Ayanz et al. 2023). The dangers related to wildfires are highly influenced by the spatial distribution of biophysical variables such as weather conditions, fuel types (vegetation composition and structure), and topographic features, which determine the spatial patterns of fire spread and intensity, while influencing along with human-related drivers, when, where and if new ignitions can turn into large-scale events (Chuvieco et al. 2023; Ganteaume et al. 2013; García-Llamas et al. 2019; Ruffault and Mouillot 2017). In addition, higher temperatures, intense drought periods, and changing precipitation patterns, based on climate projections (Jones et al. 2022), could facilitate the frequency of fire ignitions and extreme fire spread rate and intensity in the near future (Lozano et al. 2016; Molina-Terrén et al. 2019; San-Miguel-Ayanz, Moreno, and Camia 2013; Turco et al. 2018). Therefore, it is more evident than ever that suppression will frequently collapse under the manifestation of the nature of wildfires occurring in overstocked areas under the influence of climate change, alternating the fire regime by modifying fire size, frequency and burn severity (Grüning, Seidl, and Senf 2023), causing not only severe

environmental damages and economic losses but also a high number of fatalities (Cardil, Delegu, and Molina-Terrén 2017; Diakakis, Xanthopoulos, and Gregos 2016; Molina-Terrén et al. 2019).

It is widely assumed that active canopy fires represent a special challenge for foresters and fire managers, in terms of fire behavior such as rate of spread, flame length, burn probability and fireline intensity (Alexander and Cruz 2011; Finney and Grumstrup 2023; Monedero, Ramirez, and Cardil 2019). A prerequisite for active canopy fire spread is a low canopy base height that will allow fire transition from the surface to the tree crown, and high canopy fine fuel availability, coupled with dense canopy cover, to allow the sustaining of flames and spreading through the canopy layer. Once a fire reaches the tree canopies and spreads through them, a faster spread and increased energy release rate are expected because it is strongly related to the fuel structure (Or et al. 2023; Rothermel 1983). Such behavior greatly affects the efficiency of suppression actions, often exceeding the conditions considered within the firefighter safety limits (Tedim et al. 2018). Even modeling the initiation and spread of canopy fires is still considered a difficult task (Rodríguez et al. 2017).

Consequently, the structure and amount of fuel in tree canopies play a major role in defining how fire will behave if it transitions to the canopy (Scott and Reinhardt 2001), assessing wildfire hazards, potential fire severity, crown flame length and rate of spread (Marino et al. 2022). The availability of continuous and large-scale information on the spatial distribution of fuels (Rollins 2009), has shown its practicality in improving decision-making when dealing with fire suppression and fuel management problems (Moran, Kane, and Seielstad 2020). The necessity of an integrated fire related European strategy is pushing for the production of European fuel maps (Aragoneses et al. 2023), describing both the surface (understory) and overstory vegetation, that will solve the issue of a lack of harmonized forest geospatial data that will cover most of the European continent and all EU countries (Pucher, Neumann, and Hasenauer 2022). Consequently, canopy fuel maps need to be standardized at pan-European level and produced at an operational scale, considering that most of the previous fuel maps were produced at coarse scales (1 km). Thus, the current coarse maps do not fulfil the needs of EU countries for high resolution canopy fuel maps for running forest fire simulation outputs. Therefore, an innovative method using satellite data combining allometric equations can be an alternative to countries with no information on canopy fuels.

Canopy fuels are described by two key parameters, that is, the canopy base height in meters (CBH) and the canopy bulk density in kilograms per cubic meter (CBD). The CBH expresses the vertical distance along the stem from the surface to the continuous live crown fuel, considering the lowest branch of the tree crown (Finney 2004; Maltamo et al. 2020; Stefanidou et al. 2020), while the CBD describes the density between foliage biomass and canopy volume (Ruiz-González and Álvarez-González 2011; Scott and Reinhardt 2001; Wang et al. 2022) across the whole volume of the stand, not being segmented by the tree canopies, thus covering the whole plot area. In addition, canopy cover (CC), expressed in percentage, and stand height (SH) are the other two variables that are important to describe and understand the vertical arrangement and horizontal continuity of canopy fuel (Rollins 2009). All four variables are required in most fire behavior modeling algorithms, representing the characteristics of canopy fuel (Cruz, Alexander, and Wakimoto 2003; Yurtgan, Baysal, and Küçük 2022). CBH and CBD can be used to evaluate crown fire hazards and simulate fire spread and behavior with simulators such as FARSITE (Finney 2004), FlamMap (Finney 2006), FSim (Finney et al. 2011), Wildfire Analyst (Monedero, Ramirez, and Cardil 2019), or Cell2Fire_SB (González-Olabarria et al. 2023), just to mention a few of them.

Mapping the quantity, distribution, and characteristics of canopy fuels can be carried out with the support of remote sensing applications. Different sensors, passive and active, have been applied to determine canopy fuels, such as Sentinel-2A (Arellano-Pérez et al. 2018), SAR imagery (Saatchi et al. 2007), active sensors that uses a waveform instrument, such as the global ecosystem dynamics investigation (GEDI) from NASA (Aragoneses et al. 2024; Hoffrén et al. 2023), and light detection and ranging technology (LiDAR), in particular from airborne laser scanning (ALS) data (Andersen, McGaughey, and Reutebuch 2005; Chamberlain, Sánchez Meador, and Thode 2021; Erdody and Moskal 2010), being the most accurate and efficient measurement over extensive areas. Nonetheless, variables such as CBH and CBD can be estimated by ALS or from unmanned aerial vehicle close-range sensing technologies at a more local scale. The pixel size of the CBH and CBD rasters from LiDAR data can be available at high spatial resolution, between 10 and 30 m (Engelstad et al. 2019; Moran, Kane, and Seielstad 2020; Shin et al. 2018). Integration of LiDAR data and field measurements to run fire spread simulations in Spain has been successfully achieved by González-Olabarria et al.

(2012) at the local scale and by Krsnik et al. (2020) at the regional scale. Nevertheless, this approach is not suitable to cover large areas on a continental or global scale. Remote sensing products at the European or global scale, such as the tree species map (Bonannella et al. 2022), the aboveground biomass (AGB) map (Pirotti et al. 2023b), the canopy cover (Hansen et al. 2013), but especially the canopy height model (Lang et al. 2023; Potapov et al. 2021), are crucial inputs to develop CBH and CBD variables with an accurate and replicable procedure.

The spatial distribution of CBH and CBD is here derived from the latest open source, uniformized, and available data, which guarantees the accessibility to researchers and fire management-oriented technicians for two of the most relevant and challenging to spatially quantify variables associated with crown fire hazards. Such applications have become paramount across Europe in the current context of extreme climatic events e.g. summer heatwaves and prolonged droughts (Suarez-Gutierrez, Müller, and Marotzke 2023), leading to the occurrence of large and severe wildfires not only in fire-prone regions such as the Mediterranean countries but also in Central and Northern Europe (El Garroussi et al. 2024; Kudláčková et al. 2023). Integrating a common data source for CBH and CBD, as the ones provided in this work, allows for co-learning between European fire management agencies and researchers, making it possible to design and adopt strategic fire prevention plans with similar specifications across Europe, and expanding the use of fire behavior models on countries with still little fire activity and fuel modeling experience.

Considering the above, we targeted applying a cost-effective methodology to produce CBH and CBD products at a fine spatial scale, harmonizing them at the pan-European level, and combining ground acquired forest biometric data with remote sensing to improve the accuracy of the derived datasets.

The current work builds on the use of a 2020 biomass map, a tree species map, and the development of an allometric relationship to determine CBH on the one hand and extract the foliage biomass to quantify CBD on the other hand at 100 m spatial resolution. The specific steps followed, as described in the next sections of this paper, were: (i) mapping the CBH as a function of a global canopy height model, tree species probabilistic model, and through allometric relationship between total stand height and the height of live branch insertion using allometric models based on national and local data for specific tree species; (ii) extracting the foliage biomass from previous pan-European models that estimated the AGB by tree components (*e.g.*, stem, branches, foliage, etc.) based on the diameter at breast height (DBH) using the specific equation to predict foliage, and therefore, to compute the CBD model; and (iii) estimating error metrics from local studies, where the CBH and CBD were computed with LiDAR data and field measurement from four countries (Portugal, Greece, Italy, and Norway) with a higher spatial resolution.

2. Materials

2.1. Study area

The study area covered all the pan-European territory, where the canopy fuel maps were produced. This area is notably varied as it goes from Mediterranean to Nordic climate. The vegetation follows the climate variability, and we see Mediterranean ecosystems with very mixed shrub and xerophilic species to single-species forest stands with species used to colder climates. The validation process was carried out through four countries that represent such variability and that had available forest inventory plots regarding CBH and CBD: Portugal, Greece, Italy, and Norway. The vegetation in Portugal was mostly occupied by resin pine (*Pinus pinaster*), eucalyptus (*Eucalyptus* spp.), stone pine (*Pinus pinea*), cork oak (*Quercus suber*), oaks (*Quercus* spp.) and other broadleaves. In Greece, the vegetation was mainly composed of *Olea europaea* var. *Sylvestris*, *Pistacia lentiscus*, *Erica manipuliflora*, and *Myrtus communis*, while in wetter locations we found *Quercus coccifera*, *Rosa sempervirens*, *Smilax aspera*, and *Rubia peregrine*. On slopes and southern aspects, we found plant communities of *Erica manipuliflora* and *Erica arborea*, while the relatively better ecological locations were dominated by *Arbutus unedo*, *Calycotome villosa*, and *Spartum junceum*, mostly mixed with sparse *Pinus halepensis* Mill. or *Pinus pinea*. The wetter locations and northern aspects were dominated by *Quercus ilex*, *Fraxinus ornus*, *Phillyrea latifolia*, and *Quercus pubescens*. In Italy, due to the country's latitude gradient and extension over the Mediterranean, we see a situation that is similar to Greece and Portugal in the south, up to a tree species composition similar to Norway in the north. In Norway, the plots were located in boreal forests, being dominated mostly by species such as Norway spruce (*Picea abies*) and Scots pine (*Pinus sylvestris*), with the presence of some deciduous trees, typically by Birch (*Betula pendula*).

2.2. Input rasters at pan European scale

To estimate CBH and CBD in raster format, we used as inputs several global rasters reprojected to the World Geodetic System WGS84 geographic coordinate reference grid with $\sim 9 \times 10^{-4}$ degree resolution, commonly referred to as ~100 m spatial resolution maps. Figure 1 depicts the input layers and the intermediate and final maps, Table 1 also lists in a table the main input data with source, spatial resolution and date. The AGB map, a necessary precursor to derive CBD, was estimated in a previous work by the authors (see Pirotti et al. 2023b) and is detailed in the methods section.

As described in the next sections, CBH and CBD were derived from existing earth observation (EO) products. We used a canopy height map (CH) from Lang et al. (2023) that was based on deep learning with a convolutional neural network (CNN) using descriptors extracted from ESA's Sentinel-2 imagery. Training for this map was achieved by using vertical vegetation profiles from the GEDI data. GEDI is a photon-counting LiDAR instrument that collects data from April 2019 (Dubayah et al. 2020; Potapov et al. 2021), providing a high degree of accurate information depending on terrain morphology (Kutchartt, Pedron, and Pirotti 2022). The CH raster was provided at global scale at a 10 m spatial resolution for the year 2020. A raster of canopy cover (CC) from the work of Hansen et al. (2013) was also used, which is updated
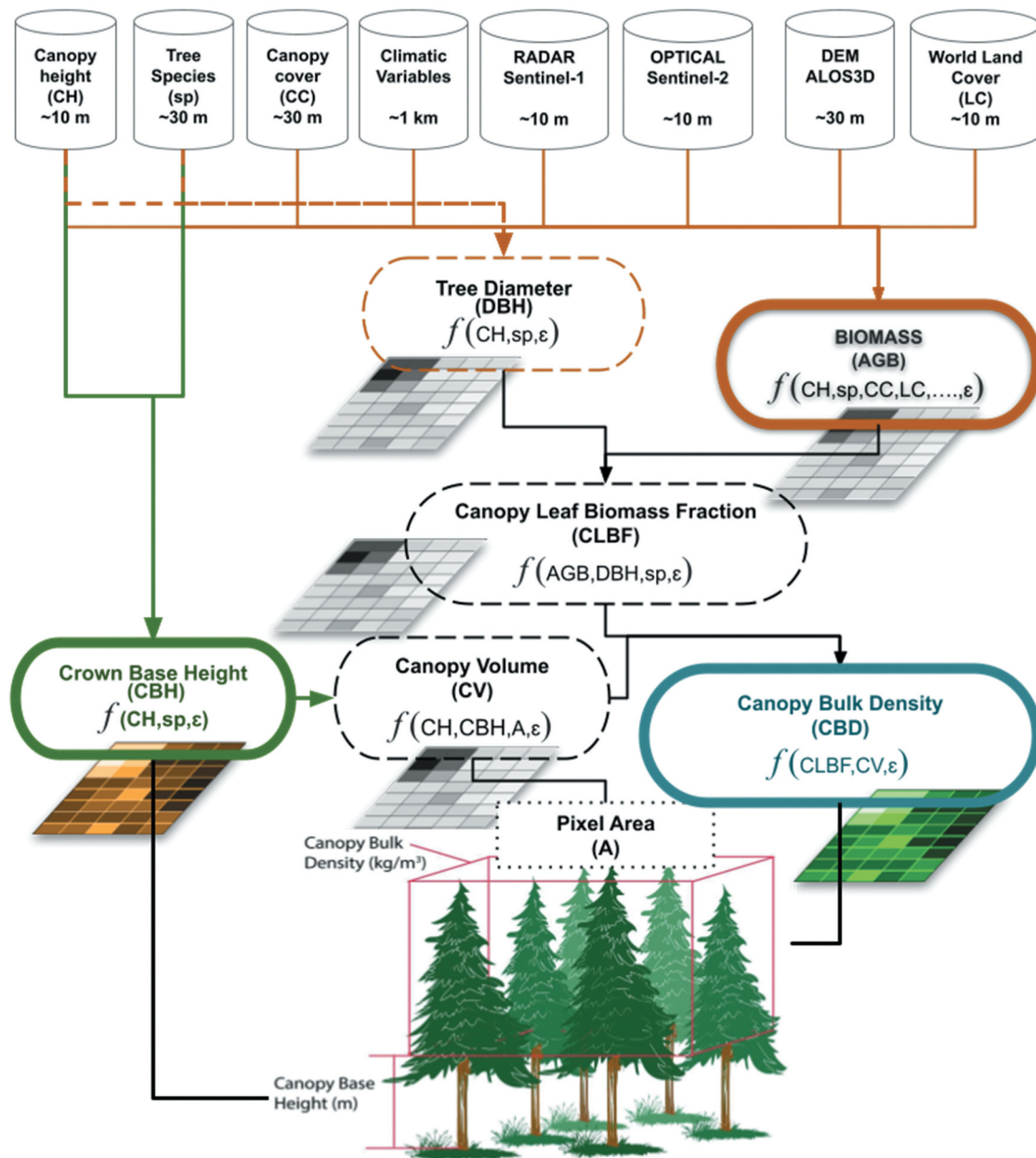
Figure 1. Workflow for combining multiple imagery sources to spatially quantify canopy base height (CBH) and canopy bulk density (CBD) using earth observation, AI, and allometric relationships.

Table 1. Spatial data input – see also Figure 1. Resolution is the original pixel size, date is the date of validity.

Input data	Original resolution* and year of validity	Reference
World Land Cover (LC)*	10 m 2018	Zanaga et al. (2021)
DEM ALOS3D*	30 m 2020	Tadono et al. (2016)
Optical Sentinel-2* Enhanced Vegetation Index (EVI) * Normalized Vegetation Index (NDVI)*	10 m 2020	Main et al. (2011)
RADAR Sentinel-1 VV+VH pol.*	10 m 2020	Pirotti et al. (2023a)
RADAR ALOS HH+HV pol.*	25 m 2020	Shimada et al. (2014)
Climatic variables*	1000 m 1990–2000	Hijmans et al. (2005)
Canopy Height (CH)	10 m 2020	Lang et al. (2023)
Canopy Cover (CC)	30 m 2000 (updated to 2020 with loss/gain mask)	Hansen et al. (2013)
Tree Species (sp)	30 m 2000–2020	Bonannella et al. (2022)

*These layers were used for the AGB map for 2020 a precursor of the CBD map as described in (Pirotti et al. 2023b), but not for the CBH and CBD estimation.

yearly. This map explains a significant degree of the variance in stand characteristics, both for the estimation of the AGB precursor map and for the final CBD map. CC refers to the portion of the ground area covered by the vertical projection of the tree crowns. The canopy cover measurement is expressed in percentages with integer values from 0 to 100. The original resolution of the canopy cover layer was 30 m and was resampled to 100 m. The percentage of the cell that is covered by high vegetation was determined by consensus, with updates based on annual cover loss and gain maps also provided by Hansen et al. (2013). The satellite data described in Figure 1 and Table 1 were collected using the Google Earth Engine framework (Gorelick et al. 2017) that is freely available for scientific research. The procedure workflow was carried out in the R environment on a cloud computing cluster with 16 available cores for processing. Table 1 below lists the reference layers that were used from earth observation products.

3. Methodology

As mentioned in the introduction, the aboveground biomass 2020 map was created using a stacked ensemble of machine learners (Pirotti et al. 2023b) by combining multiple imagery sources such as canopy height, canopy cover, active sensors (radar backscatter median annual values from Sentinel-1 and ALOS-2), optical sensors (annual composite of Enhanced Vegetation Index (EVI) and Normalized Difference Vegetation Index (NDVI) obtained from Landsat-8), land cover maps, a digital elevation model (DEM), and 19 bioclimatic variables from Fick and Hijmans (2017). All input layers added up to 49 covariates that were used for training an artificial intelligence (AI) framework consisting of a stacked ensemble of machine learning algorithms. The AI framework used is an H2O cluster (2022) accessed via the R environment. The training and testing data used for this approach comes from an existing 2018 AGB map (Santoro and Cartus 2021; Santoro et al. 2022). The distribution of AGB values is unbalanced with higher frequencies in lower values. To address this issue the training and testing data were sampled using stratified sampling after dividing possible AGB values in 7 strata, each with a range of 50 Mg ha^{-1} over the overall range from less than 50 Mg ha^{-1} to 300 Mg ha^{-1} or above.

The training dataset was used to train a stacked ensemble of machine learners in an AI framework over subdivisions of Europe. Europe was divided in tiles to limit the variability and make sure that the final models are more regional-oriented. Testing and training data were independent. Prediction of the test dataset resulted in an overall RMSE of 32.4 Mg ha^{-1}. The full details are provided in the work by authors in (Pirotti et al. 2023b). This biomass map was used as key input for the canopy bulk density map as can be seen in the pipeline depicted in Figure 1.

3.1. Allometric models

Allometric equations were used to estimate and map both canopy fuel maps (CBH and CBD). Inputs for

calculating CBH and CBD include tree heights, canopy volume, and the foliage fraction of the AGB (Figure 1). As mentioned, tree height was available from the work by Lang et al. (2023), while canopy volume and foliage fraction were estimated as products through allometric relations. These relations are species-dependent, in the sense that a different equation must be solved and applied for each tree species considered (see Figures S1 and S2 and Tables S1 and S2 in the appendix). To assess which equation to use at each cell, a 30 m resolution European tree species map was assigned and used just to compute the canopy fuels (Bonannella et al. 2022). This map represents the probability of the presence of the following 16 tree species: *Abies alba* Mill., *Castanea sativa* Mill., *Corylus avellana* L., *Fagus sylvatica* L., *Olea europea* L., *Picea abies* L.H. Karst., *Pinus halepensis* Mill., *Pinus nigra* J.F Arnold, *Pinus pinea* L., *Pinus sylvestris* L., *Prunus avium* L., *Quercus cerris* L., *Quercus ilex* L., *Quercus robur* L., *Quercus suber* L., and *Salix caprea* L. This map provided the realized distribution of these 16 tree species using 300 variables as independent covariates to feed an AI framework. The training was done using more than 2.5 million trees located in Europe and obtained from different open-access databases. The Global Biodiversity Information Facility (GBIF) and data from national forest inventories from multiple EU member states published by Mauri, Strona, and San-Miguel-Ayanz (2017) were used.

Species-specific allometric equations were developed to estimate two specific variables: the CBH and the foliage fraction that is necessary for the CBD map. The rationale is that CBH depends on the silvicultural management, age, and biosocial status of the tree at a specific stand density (Maltamo et al. 2018). Foliage fraction is also correlated with the above-mentioned factors, with tree species explaining a lot of the variance in the models as well, depending on the amount of overlapping between crowns in the vertical canopy profile, based on tree height and crown ratios (Ex et al. 2016). Mapping microclimatic and local ecological factors are also partly correlated to foliage fraction, but mapping such values at the pan-European scale is out of the scope of this work. It would add unnecessary complexity and the foreseen improvement of the model is marginal. The model thus focuses on using solely tree species, which explain a large part of the variance of foliage fraction values.

The species maps provide a value of probability for each species to be present at a certain node. Naturally, the probabilities could add to values above 1, as any

area can potentially have a high probability of hosting more than one tree species. The allometric models were therefore calculated for all species, and then the occurrence probability was used as a weight after normalization – *i.e.*, the probability of all species adding up to 1 for each cell.

3.2. Canopy base height (CBH) mapping

Canopy base height, also known as branch insertion height, is the vertical distance from the ground to the first branch of the tree (Figure 1 bottom sketch). To compute the CBH map, species-dependent allometric models were fitted with observed ground data of tree height and CBH across Europe for 16 tree species, as in equation 1:

$$CBH = f\left(CH, sp, \varepsilon\right) \tag{1}$$

where CH is the canopy height, *sp* is the raster dataset depicting the tree species probability as described in the previous section, and ε is the error of the model. Species-specific relationships between the tree height and the branch insertion height were obtained through fitting models using more than 85,000 inventoried trees. These trees were distributed among different countries, at national scales or from local studies conducted in Spain, Portugal, Italy, Norway, and Germany (Alberdi et al. 2017; Mihajlovski et al. 2023; Schindler et al. 2023). The least trimmed squares robust (LTS) regression algorithm was used for fitting the linear model. This specific procedure limited the impact of some outliers and other deviations from the standard linear regression model, minimizing the sum of squared residuals compared to classical least squares estimators (Pison, Van Aelst, and Willems 2002; Rousseeuw 1984). The LTS regression method minimizes the sum of the smallest squared residuals and is defined as:

$$\hat{\beta}(LTS) = \operatorname{argmin} \beta \varepsilon Rp \sum_{i=1}^{h} r_{[i]}^2(\beta) \tag{2}$$

where $r_{[i]}^2(\beta)$ represents the square of the residual of the ith point, *i.e.*, $y_i\text{-}\beta^T X_i$; h is the cardinality of the points used, usually $h = n/2$; in other words half of the observations that have the smallest residual are used. This is of course an iterative process.

Table S1 in the appendix shows that the number of trees used for fitting the species-specific models to predict the branch insertion height ranged from 224 to > 20,000, reporting the error metrics through a *k*-fold cross-validation method such as the R-squared, the root mean square error (RMSE),

and the mean absolute percentage error (MAPE), as shown by Sileshi (2014) and Kutchartt et al. (2021).

3.3. Canopy bulk density (CBD) mapping

Canopy bulk density is defined as "the mass of available canopy fuel per canopy volume unit" (Van Wagner 1977), commonly expressed in kilograms per cubic meter. The canopy volume (CV) is defined using the difference between canopy height and CBH (Figure 1 bottom sketch). In this work, we defined bulk biomass as the thin biomass (AGB_{thin}), identified as the fraction of the AGB consisting of leaves. We can therefore map each cell with the following generic formulas:

$$CBD = AGB_{thin}/CV \tag{3a}$$

$$AGB_{thin} = f(DBH, AGB, sp, \varepsilon) \tag{3b}$$

$$CV = CH - CBH \tag{3c}$$

$$DBH = f(CH, sp, \varepsilon) \tag{3d}$$

where AGB_{thin} is the thin biomass (Mg ha^{-1}) which is a fraction that depends on the overall AGB, CV is the canopy volume, CH is canopy height (m), DBH is the diameter measured at breast height (1.3 m from the ground) and by the species presence (sp) and through the error (ε) of the model used.

So, the overall CBD is a function of all the above and can be expressed as:

$$CBD = f(DBH, AGB, CBH, sp, \varepsilon) \tag{4}$$

The AGB was allocated by tree components, extracting the foliage biomass according to the equations provided by Forrester et al. (2017b) at the pan-European level. The models selected used power law functions, based only on DBH as an explanatory variable (see all the equations used in Table S3 in the appendix). The fraction of foliage biomass was divided by the canopy volume using a mattress figure based on the CBH layer. It means that all the full area of the pixel was used, and it was not segmented by individual tree crowns. Therefore, the first step was to define the volume of the canopy in each cell in the grid, then to obtain the fraction according to the foliage mass, which decreases as the trees increase in diameter. We combined the equations for foliage biomass and total aboveground biomass to get the fraction allocated by foliage. The results of the percentages and how they change depending on DBH are

shown in Table 2. However, not all the tree species were covered by species-specific allometric equations. Therefore, the missing species were covered by general or multi-species models, considering the leaf type by broadleaves and conifers or by similarity of species. Consequently, for species such as *C. avellana*, *O. europaea*, and *S. caprea*, the general broadleaves model was applied, while *A. alba* was replaced by the general conifers model. On the other hand, *P. halepensis* was replaced by *P. abies*, *P. pinea* by *P. sylvestris*, and the two oaks missing (*Q. cerris* and *Q. suber*) were repealed by the *Q. robur* model. These models were crucial to extracting the foliage mass from the total AGB.

Diameters at breast height, which are necessary for the allometric equations provided by Forrester et al. (2017b), were estimated using allometric equations that allow for the estimation of DBH from tree heights. The independent variable is the canopy cover height, which is available as an Earth observation product with a pixel size of 10 m (Lang et al. 2023). An inverted allometric relationship (equation 3) was obtained using an open database from Aussenac et al. (2023), which included the DBH, height, and tree species for 42 million trees distributed in three European landscapes (France, Poland, and Slovenia). In addition, data from the Italian National Forest Inventory (Gasparini et al. 2022) was integrated into these models (see Table S2 in the appendix). Therefore, these models allowed us to estimate the DBH as a function of the tree heights and, thus, to predict the foliage mass and compute the CBD. In short, both for the estimation of the diameter based on the height as an independent variable and the estimation of the foliage biomass based on the DBH, multiplicative models, also known as a power law equation, were used:

$$y = X^{\beta_1} e^{\beta_0} \tag{5}$$

where y is DBH, the response variable, β_0 and β_1 are the model parameters estimated by ordinary least squares (OLS), and X is the independent variable, the tree height.

3.4. Accuracy metrics

All models from the allometric equations and the final maps were validated through accuracy metrics. The equations and validation metrics considered in this work were the following:

Table 2. Foliage biomass fraction (%) of the 16 tree species according to different diameter at breast height (DBH) values in cm.

DBH (cm)	Abies alba	Castanea sativa	Corylus avellana	Fagus sylvatica	Olea europaea	Picea abies	Pinus halepensis	Pinus nigra	Pinus pinea	Pinus sylvestris	Prunus avium	Quercus cerris	Quercus ilex	Quercus robur	Quercus suber	Salix caprea
5	13.7	1.5	5.2	2.7	5.2	20.5	11.2	24.1	9.4	9.4	0.7	5.5	4.8	6.4	5.5	5.2
10	10.3	1.6	3.6	2.1	3.6	16.0	10.6	12.7	6.7	6.7	0.4	4.4	4.3	4.5	4.4	3.6
20	7.6	1.7	2.5	1.6	2.5	12.3	10.1	5.8	4.7	4.7	0.3	3.5	3.8	3.2	3.5	2.5
30	6.4	1.7	2.0	1.4	2.0	10.5	9.8	3.5	3.8	3.8	0.2	3.0	3.6	2.5	3.00	2.0
40	5.6	1.8	1.7	1.2	1.7	9.4	9.6	2.4	3.3	3.3	0.2	2.7	3.4	2.2	2.7	1.7
50	5.0	1.8	1.5	1.1	1.5	8.6	9.4	1.7	2.9	2.9	0.2	2.5	3.3	1.9	2.5	1.5
60	4.6	1.8	1.4	1.0	1.4	8.0	9.3	1.4	2.7	2.7	0.1	2.4	3.1	1.7	2.4	1.4
70	4.3	1.8	1.3	0.9	1.3	7.5	9.2	1.1	2.4	2.4	0.1	2.3	3.1	1.5	2.3	1.3
80	4.1	1.8	1.2	0.9	1.2	7.1	9.1	0.9	2.3	2.3	0.1	2.2	3.0	1.4	2.2	1.2
90	3.8	1.9	1.1	0.8	1.1	6.8	9.0	0.8	2.1	2.1	0.1	2.1	2.9	1.3	2.1	1.1
100	3.7	1.9	1.0	0.8	1.0	6.5	9.0	0.7	2.0	2.0	0.1	2.0	2.9	1.2	2.0	1.0
150	3.0	1.9	0.8	0.8	0.8	5.5	8.7	0.4	1.6	1.6	0.1	1.7	2.7	1.0	1.7	0.8

$$R^2 = 1 - \frac{\sum_{i=1}^{n} (y_i - \hat{y}_i)^2}{\sum_{i=1}^{n} (y_i - \bar{y}_i)^2} \qquad (6)$$

$$RMSE = \sqrt{\frac{1}{n} \sum_{i=1}^{n} (y_i - \hat{y}_i)^2} \qquad (7)$$

$$MAPE^* = \frac{100}{n} \Sigma \frac{|y_i - \hat{y}_i|}{(y_i + \hat{y}_i)} * 2 \qquad (8)$$

where n is the number of values used to calculate the accuracy, y_i is the observed value, $\hat{y}_i$ is the predicted value, and $\bar{y}_i$ is the mean value. Mean absolute percentage error (MAPE*) is slightly modified from the common MAPE formula in that in the common formula the reference is the observed value, which in our case can (and often is) equal to zero in the case of CBH, as it is common to have canopies reaching the ground. The MAPE will not provide reasonable values when the denominator is zero or very close to zero. We therefore addressed this issue by using the arithmetic mean of observed and predicted values in the denominator, as in Miller (2011).

3.5. Uncertainty estimation

Uncertainty quantification via the propagation of known errors is of primary importance for making data-driven decisions. Estimating corresponding uncertainties for the mapped canopy fuels provides corresponding uncertainty maps with expected deviations from the estimated values. This is especially important in mapping variables that are calculated using multiple inputs, each with its own intrinsic error distribution. In this work, we used two different approaches for the two datasets. CBH estimation is a mathematically simpler composite function, and uncertainty can be calculated using the calculus-based chain-rule:

$$\Delta CBH_i = \sqrt{\left(\frac{\delta cbh}{\delta h} \Delta h\right)^2 + (e_i)^2} \qquad (9)$$

The uncertainty of CBH (ΔCBH) estimated for the ith species includes the uncertainty of the species map (Ei), the uncertainty of the model for the ith species (Ei) expressed with its RMSE, and the uncertainty of the canopy height map (Δh) provided by Lang et al. (2023). We assume no correlations and independence of variables.

Regarding CBD, the number of functions embedded in the composite function makes the calculation of error propagation more complex, so we adopted Monte-Carlo (MC) simulation. Also, in this case, we assume no correlations between variables, independence of variables, and normally distributed error. The Monte Carlo procedure consists of iterating over a random estimate of the expected error using the known accuracy metrics. In this work, we used 380 iterations. Notably, MC simulations use a very high number of iterations, from one to two orders of magnitude, but due to the very large data volume for each raster layer, that is, 3.20×10^9 pixels, those numbers were not feasible with the computing infrastructure that was used in this work. We therefore based the number of iterations on the following relationship (Hauck and Anderson 1984) that relates the number of iterations with the required convergence. Let E_1, E_2, ... E_n be the errors that are independent and follow an identically distributed random distribution with a finite mean μ and variance σ^2. Let $\bar{\varepsilon}$ be the average of the sample and s the standard deviation of the sample. The Central Limit Theorem states that the mean of a sample is normally distributed regardless of the type of distribution of the population from which the samples were taken, if the population is significantly larger than the number of samples. The confidence interval (CI) that is set as the target can be calculated with the well-known formula:

$$CI = \left[-z \cdot \frac{s}{\sqrt{n}}, +z \cdot \frac{s}{\sqrt{n}} \right] \qquad (10)$$

where n is the number of samples, $\bar{\varepsilon}$ and s is the mean and standard deviation of the samples. The z statistic is the critical z-score value when using a specific confidence/significance level; it is approximately -1.96 and $+1.96$ in the case of a 95% confidence level (alpha $= 0.05$ significance level). Equation (10) is derived from the confidence interval's probabilistic form and can be rearranged by substituting z in terms of a specific level of precision φ. Then we obtain the following equation in probabilistic form:

$$P\left(-\frac{\varphi}{s/\sqrt{n}} < \frac{\mu}{s/\sqrt{n}} < \frac{\varphi}{s/\sqrt{n}} \right) = Confidence\ Level$$
$$(11)$$

At this point, we can estimate the number of simulations required for a desired confidence interval (level of precision) by solving the upper and lower bounds of equation (11) for the only unknown variable n. There seem to be two unknowns, n and s; however, s- the sample standard deviation, can be obtained by iterating a number of times. We can therefore estimate the number of iterations needed as we consider one sample for each iteration with the following expression:

$$n = [Z_{CI} \cdot S/E]^2 \qquad (12)$$

where n is the number of iterations needed, S is the estimated standard deviation of the output, E is the desired margin of error, and Z_{CI} is the critical value of the normal distribution for a specific CI, *i.e.*, the z value such that the area of the right-hand tail in a normal distribution is $\alpha/2$ where α is. It is the number that satisfies $P(Z>z\alpha/2) = \alpha/2$, where Z follows a normal distribution with a mean of 0 and a standard deviation of 1. $CI = \alpha/2$ can be found by setting the desired confidence level equal to $100*(1-\alpha)$ and solving for α. So, if we would like to simulate our error metric at 95% confidence within 10% of the expected standard deviation s of the error values, as a rule of thumb, we would need 380 iterations $[1.96 * s/(s * 0.1)]^2 = 380$. In all cases, error metrics had to be aggregated by pixel size. This was done with the following procedure:

$$U = \sqrt{\frac{1}{N} \sum_{i=1}^{n} w_i u_i^2} \qquad (13)$$

where w is the weight of the area fraction inside the pixel at final resolution, *i.e.*, 100 m, and is equal to 1 if the smaller pixel is completely covered by the final-resolution pixel, < 1 otherwise. N is the number of pixels that overlap the full-resolution pixel.

4. Results

4.1. Canopy base height mapping

The resulting allometric models, created for calculating CBH, are available in Table S1 in appendix with their corresponding accuracy metrics. The models were used to estimate the final pan-European CBH map depicted in Figure 2 (left), and accuracy metrics were embedded in the error propagation to assess the relative uncertainty map in Figure 2 (right). The number of samples by species was heterogeneous, considering a range between 224 and 21,913 measurements, but well distributed among countries from different latitudes. The metric errors were quite similar between tree species, with only four species exceeding 10% in MAPE, providing satisfactory results for the CBH prediction.

Figure 2 also shows the locations where the validation data were obtained. Predominantly, the highest CBH values were concentrated in the alpine regions, specifically in countries such as Switzerland, Austria, and Northern Italy, but also in regions of Eastern Europe. Notably, high CBH values were related to high uncertainties, with RMSE between 6 and 8 m (Figure 2 – right). High RMSE values were also evident in boreal areas, where CBH values were not extremely high but had much higher uncertainties.
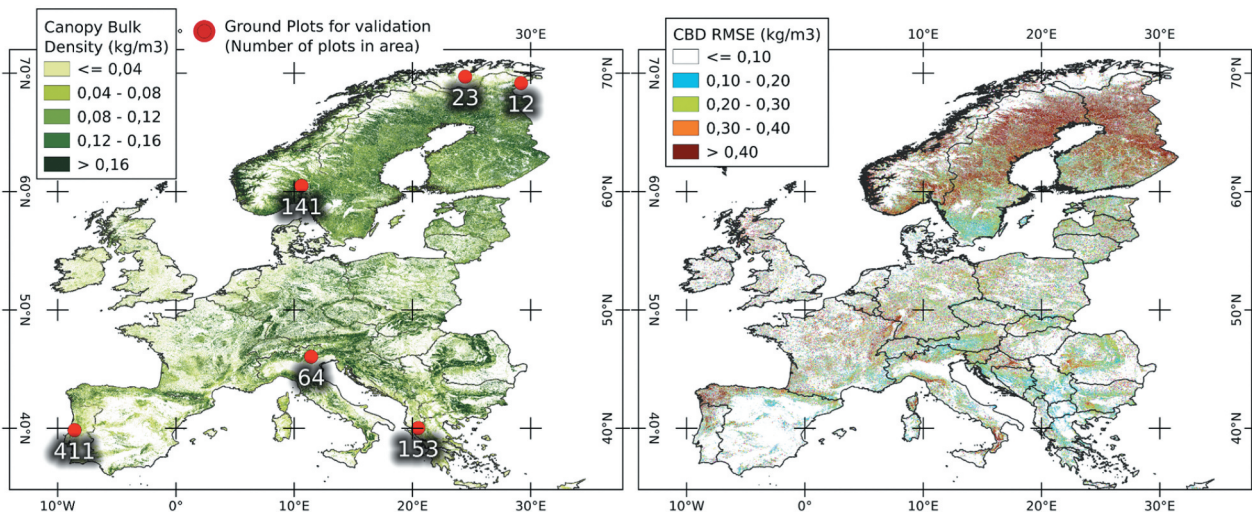
4.2. Canopy bulk density mapping

Canopy bulk density depends on the fraction of thin biomass (mainly foliage) and the volume filled by the canopy. Regarding the fraction of foliage biomass, Table 2 shows the percentage of expected biomass in the foliage from the total per DBH class. This is used to assign the foliage biomass and extract the CBD dataset, shown in Figure 3. Normally, trees, especially conifer species, concentrate a high percentage of foliage biomass when they are young, but this fraction starts to decrease over time (Portsmouth et al. 2005). In this case, species such as *Abies alba*, *Picea abies*, *Pinus halepensis*, and *Pinus nigra* show high CBD values at young growth stages, and therefore, these values are strongly related to the species composition in which CBD is measured.

4.3. Validation

The validation of CBH and CBD maps was carried out using a completely independent data source consisting of two datasets: (a) 804 ground plots from across Europe, and (b) seven LiDAR-based canopy fuel maps from surveys in the same year as the canopy fuel maps.
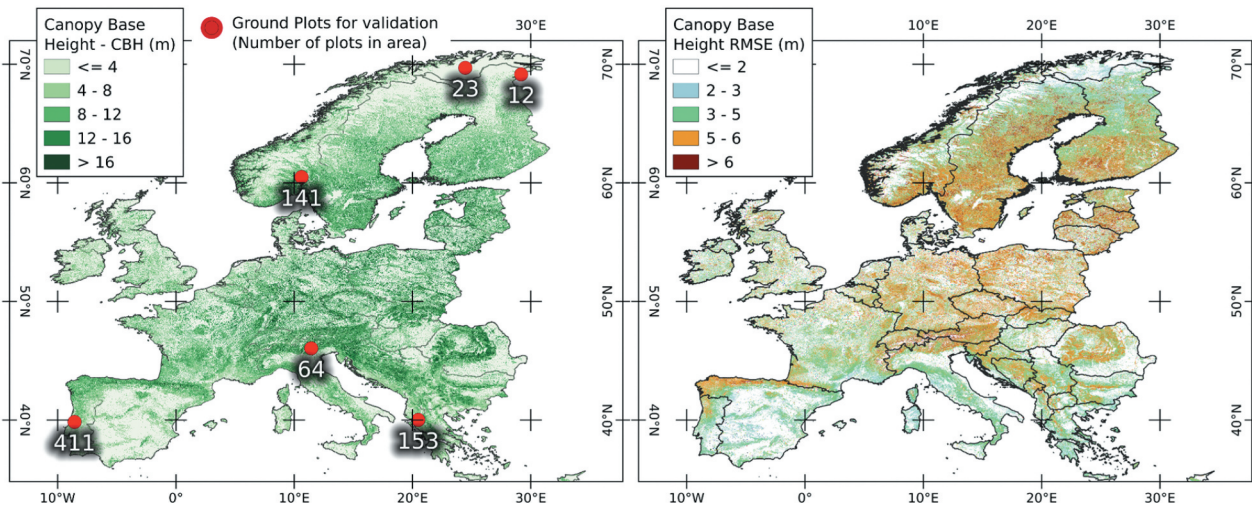
Figure 2. Left: CBH map with approximate locations of ground samples (red dots) and number of ground plots (number under the red dot) used for validation. Right: uncertainty map expressed as estimated absolute RMSE.


Figure 3. Left - canopy bulk density dataset with locations (red dots) and number of ground plots (number under the red dot) used for validation of results; right - uncertainty values expressed as estimated absolute RMSE.

4.3.1. Ground measurements

The 804 ground plots were used from four countries that provided CBH and CBD georeferenced data from field measurements: Greece (153 plots), Italy (64 plots), Norway (176 plots), and Portugal (411 plots). Canopy fuels in the field were measured in different years, between 2010 and 2020. To avoid including parts that were subject to some kind of forest disturbance, we used the Hansen et al. (2013) canopy cover loss map as a mask to remove any pixels that were detected as having had a canopy loss between the years 2000 and 2020. The approximate position of the ground plots is visible in the left quadrant of Figures 2 and 3. All ground plots, except one, which is a 1-ha square, are circular with a 10 to 20-m radius and an

area between 314 and 1,256 m^2. It should be noted that this makes a much smaller sample than the cell size of the raster, which is approximately 10,000 m^2 (1 ha). This will have an effect on results, as for example, a cell might be half covered with very dense canopies (thus high CBD values) and half covered with very light canopies, and the sample might fall completely in one of the two cases, thus not reflecting the whole area. To partially mitigate these cases, accuracy metrics were calculated using all plots and also by removing plots that fall in cells that have a forest cover of less than 80%. Figures 4 and 5 show the results and the respective accuracy metrics, where the scattering of points shows a clear concentration between 5 and 10 m in the case of CBH and between
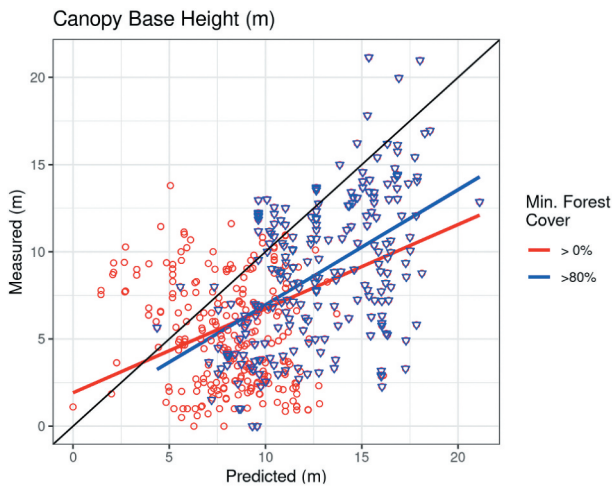
Figure 4. Ground validation for canopy base height measured from all ground samples (red) and on ground samples falling over a raster cell with forest cover equal to or above 80% (blue). Specific accuracy metrics for both are reported in Table 3.
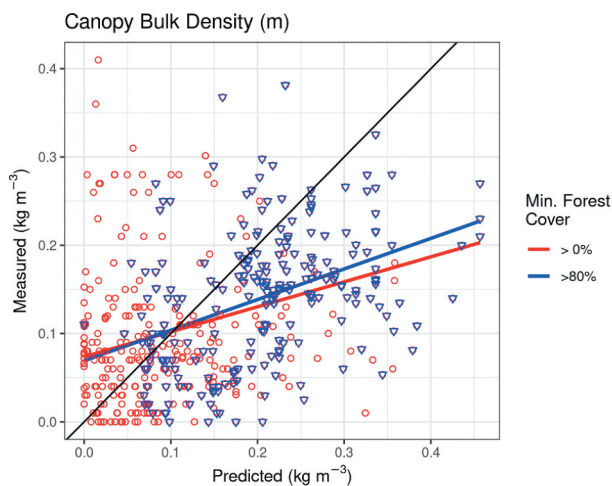
Figure 5. Ground validation for canopy bulk density measured from all ground samples (red) and on ground samples falling over a raster cell with forest cover equal or above 80% (blue). Specific accuracy metrics for both are reported in Table 3.

Table 3. Results from the ground plots shown in Figures 4 and 5. CBH units are meters, CBD units are kg m^{-3}.

Canopy Fuel Forest Cover	CBH		CBD	
	Fc > 0%	Fc>80%	Fc > 0%	Fc>80%
N	804	322	486	225
RMSE	3.9	3.8	0.099	0.085
MAPE	61%	50%	76%	59%
R	0.445	0.524	0.330	0.457

0.0 and 0.1 in CBD. It is important to note that when considering forest cover of 80% or higher (Figures 4 and 5 – right panels), the error metrics drop considerably.

4.3.2. LiDAR-derived canopy fuel maps

Further validation was done using seven canopy fuel maps with CBH and CBD, located in Portugal, which were estimated using field samples and LiDAR data with a flight between 2020 and 2021 (Mihajlovski et al. 2023). Data were combined with field measurements obtained through forest inventory in the same period. Final raster maps have a 25 m cell resolution and explain the variability of CBH and CBD with relative RMSE of 13.4–48.7% and 5.9–23.0%, respectively (Botequim et al. 2019). These areas represent a mapped estimation of CBH and CBD based on calibration using ground plots and thus provide further sources of validation for our results. Figure S3 shows the areas for visual comparison.

This information has been visually compared with the results obtained through earth observation, artificial intelligence, and allometric equations applied in this investigation that cover the pan-European scale at 100 m spatial resolution.

5. Discussion

Through this new methodology, we combined harmonized allometric equations by tree components at the EU level provided by Forrester et al. (2017b), taking into account the probabilistic tree species map provided by Bonannella et al. (2022) to gain spatial variability and specificity. This approach shows an effort to harmonize databases to develop allometric equations to predict height branch insertion and biomass equations to extract foliage biomass component, combining different sensors and validating the pan-European model of CBH and CBD through ground-truth data obtained in four different countries. Other efforts on developing superficial fuel maps were carried out by Aragoneses et al. (2023) and by the same authors for forest canopy fuel parameters at European scale Aragoneses et al. (2024), being the first harmonization at the EU level. For this reason, the main effort was to improve and solve the issue of a lack of standardized field data in the EU (Alberdi et al. 2016), where data at the national level is measured by country-specific conditions, inventory traditions and information needs (Gschwantner et al. 2022). On the other hand, most of the National Forest Inventories (NFIs) have been focused on measuring forest parameters, species composition, and sometimes health indicators, neglecting important variables such as CBH to prevent forest fires. In this regard, Spain has been one of the first countries in the EU to integrate the canopy variables related to crown fire in the last NFI, which was

adapted to the new challenges in the forestry sector of the country (Alberdi et al. 2017).

Testing the accuracy of CBH and CBD datasets at this scale is a challenging task due to the difficulties of having accurate field measurements available. In this work, it was achieved using 804 ground plots distributed across Europe and six areas with field-calibrated CBH and CBD values from 2020 LiDAR data, which were combined with field measurements at close dates. The field plots were measured in various instances between 2010 and 2020; we assume that areas without specific forest disturbance have undergone changes with CBH and CBD values well under the precision level requested by this work. As mentioned in the validation section of the results, ground plots have a much different scale and catch only a small fraction of the raster cell area, around 12%, considering a typical 20 m radius plot against the approximate one-hectare area of the cell (see Pirotti et al. 2023b). Therefore, comparing such different scales must be done with caution and should consider within-class variability vs. boundary effects; this concept is well illustrated in the work of Latty et al. (1985) and Hsieh, Lee, and Chen (2001). A more correct approach, but trivially very time-consuming and expensive, would be to sample large plots that cover the full raster cell footprint plus a buffer to account for uncertainty in the geo-positioning of the pixel. This would mean sampling plots well larger than one hectare, at least so that a down-scaling can be carried out, reaching pixel size at 30 m to better fit the plot captured on the field and compare with the data obtained from EO. Although the main issue is that field data in a high accuracy and well distributed on a pan-European scale, it is only available through the national forest inventories, where circular plots are available at much smaller sample sizes, between 250 m^2 and ~1000 m^2 (Breidenbach and Astrup 2012; Eid, Gobakken, and Næsset 2004; Fridman et al. 2014; Gobakken and Næsset 2008). Another source of uncertainty internal to the validation procedure is that the approximate 100 m cell with predicted CBH and CBD might cover a forest with high structural variability, and the ground sample might catch this variability only partially if the sampling protocol applied is flexible and does not strictly require the samples to be allocated in homogenous landscapes (Gobakken and Næsset 2008). This limitation is visible in the results shown in Figures 4 and 5, where accuracy improvements were recorded after sub-setting data from pixels with almost full (>80%) canopy cover. The improvement in MAPE is stronger for CBD, as expected considering that CBD has a biomass

component (foliage), which is directly impacted by varying degrees of canopy cover, whereas CBH does not. By sub-setting the data, we limit potential variability inside the pixel area. It is worth emphasizing that the canopy fuel metric values in each pixel are an estimated average of what is in a one-hectare area around the raster cell center. In one-hectare, there can be a very mixed scenario, with a forest with very high CBD in half a pixel and bare ground in the other half. A sample plot in the forested part of this scenario will provide the forest CBD, but the pixel will provide a value that is mixed, *i.e.*, half the plot's CBD value due to half of the pixel having no forest.

Another aspect to highlight is that training and validation AGB data were actualized from the 2018 AGB map (Santoro and Cartus 2021; Santoro et al. 2022) to 2020 by removing any sampled values that correspond to an area that had forest loss or significant gain according to the loss/gain mask of Hansen et al. (2013). This mask is available up to 2022 at the time of writing, and allows to keep only AGB values that are consistent between 2018 and 2020. It can be noted that in 2 years there can be an increase in biomass, but this factor was ignored in this work for two reasons: it will not significantly change in only 2 years except in very productive areas, and it is not possible to update consistently with enough detail considering local factors affecting tree growth. These factors are many, e.g. tree species, density, age, soil type and soil depth, climate, height of terrain, and also vary spatially. Updating without due consideration of those factors would only add more error than the expected advantage. We therefore kept the 2018 values, accepting a potential slight underestimation.

A noteworthy aspect is that the presented method has not in any way been trained against the ground plots used for validation, which are completely independent. This supports further investigation into the likely hypothesis that some training on ground plots can lead to a significant improvement in modeling performance. This would, of course, require time-consuming data collection from a wide variety of agencies and public bodies around Europe, but there is evidence that they could significantly improve the results, providing a hybrid approach that requires less training data and leads to better results.

Results in Figure 6 show a clear overestimation in canopy base height and underestimation of CBD. The two things are related as CBD partly depends on CBH, and underestimation of CBH leads to underestimation of the canopy volume (see CV in equations 3a-3d). This observation leads to two reasonable considerations: (1) the models fitted for deriving CBH (Figure S1 in appendix) are generic for all of Europe, and thus
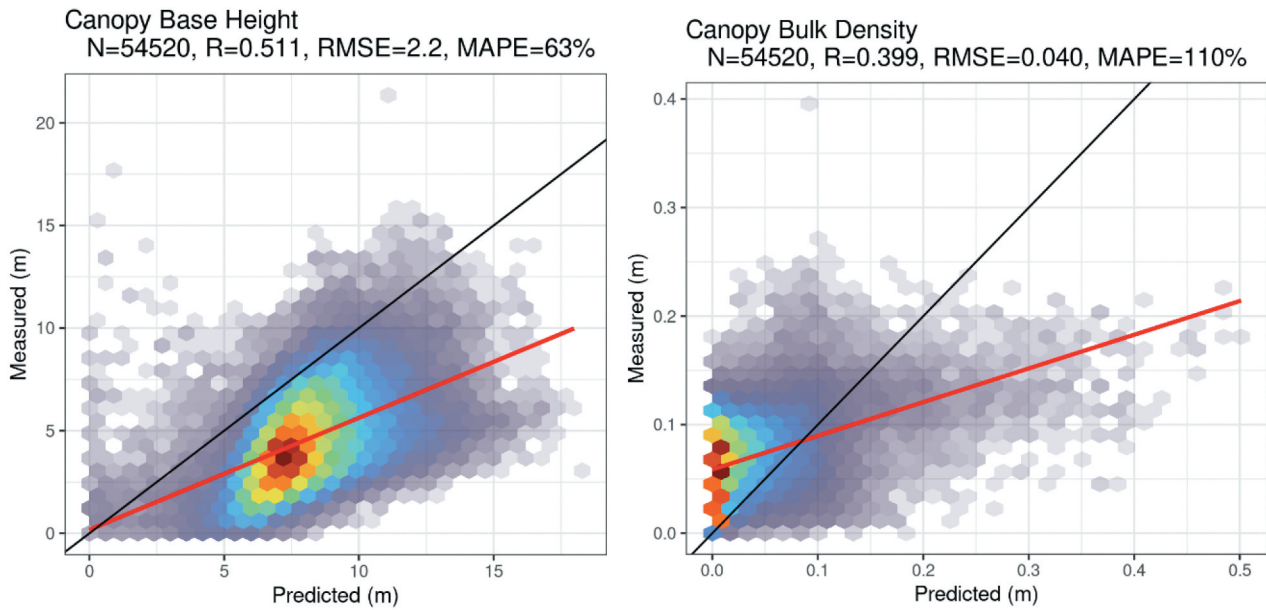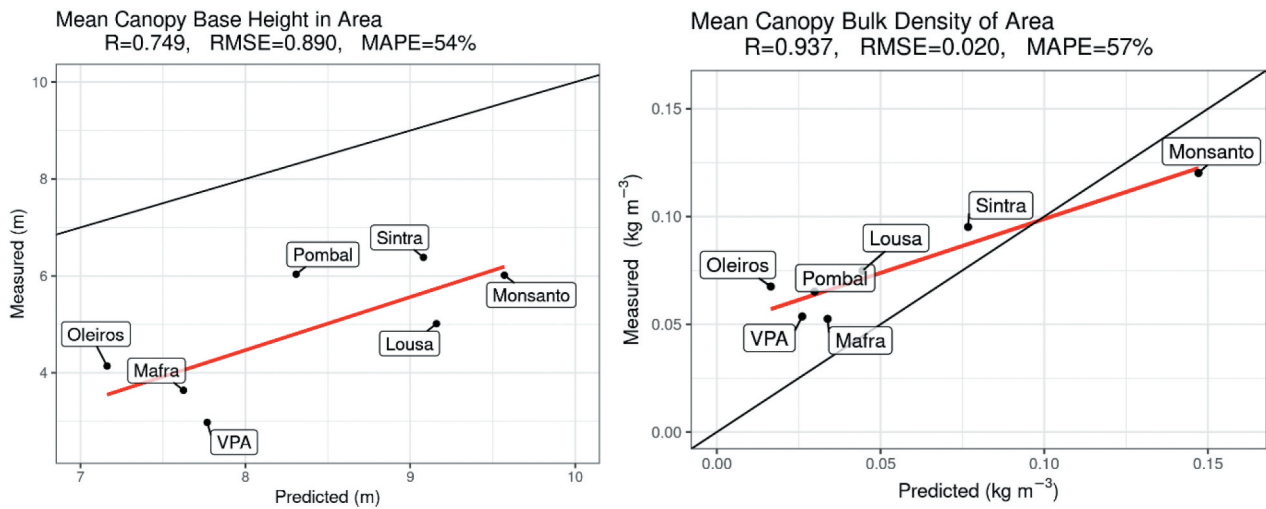
Figure 6. Binned scatterplots of predicted values in the pan-European map and observed values for each cell in the LiDAR-derived CBH and CBD maps. Specific accuracy metrics are reported in the main title.

cannot represent site-specific canopy characteristics, such as the LiDAR-derived validation sites, and (2) the LiDAR-derived method overestimates CBH. This leads to calling for a harmonized methodology for defining CBH values using a more standard method, as, for example, LiDAR is also known to consider understory as canopy, as it is extremely hard to separate low canopies from high undergrowth from a point cloud. This would naturally lead to underestimating the CBH in the LiDAR-derived values. Of course this is an open question that is worth further investigation.

LiDAR surveys are widely used to monitor forests and provide 3D point clouds. They are an ideal type of data for analysis of the vertical structure of vegetation, including CBH and CBD (Arkin et al. 2023; Botequim et al. 2019; Rocha et al. 2023). Using CBH and CBD estimated from models that use LiDAR surveys might also prove to be a valid alternative to improving accuracy by training a more accurate model of a pan-European map at one-hectare per pixel using such results. The uncertainty sources in the input data had to be considered. The canopy height map is provided with its uncertainty raster, which is propagated to the final CBH and CBD values. In this sense, it is important to address the higher degree of uncertainty at higher latitudes (e.g. Scandinavian region), as the canopy height map was trained through GEDI data, which is notably not available over ±51.6 degrees north latitude (Lang et al. 2023). Also, from the work developed by Kutchartt, Pedron, and Pirotti (2022), it can be noted that mountain areas with steep slopes

will have a high probability of very significant errors. We can conclude that areas in mountainous environments and/or at high latitudes will have more pronounced uncertainties.

Another important variable used in mapping that inherently has a certain degree of uncertainty is the species distribution probability map that has been provided by Bonannella et al. (2022). The use of species distribution is one of the most relevant aspects of the mapping process and allows for a higher level of specificity when extrapolating structural and biomass allocation. Misinterpretation of tree species presence, which is a common issue, especially in mixed stands, is due to the similarity in morphology among tree species (Hemmerling, Pflugmacher, and Hostert 2021; Pittman and Hu 2023; Torabzadeh et al. 2019). This misclassification will result in the wrong allometric model being applied for CBH estimation based on canopy height values applied to the wrong species-species model, which will thus cascade to the final CBH estimations. The same principle is applied to extract the foliage biomass from the total AGB using the wrong species-specific model, and thus, the estimation of the CBD is highly influenced by the accuracy of the tree species map. As it is trivial to state that higher accuracy in input maps will automatically define better down-stream CBH and CBD values, it should be noted that accurate and harmonized tree species real-distribution maps at the European scale with comparable resolution are not available. It was assumed that site characteristics or relations between

Figure 7. Scatterplots of predicted values in the pan-European map and observed values aggregated for each area in the LiDAR-derived CBH and CBD maps. Specific accuracy metrics are reported in the main title.

tree species would influence how tree or stand structure would evolve (Forester et al. 2017a). Resolution of several kilometers is available (Mauri, Strona, and San-Miguel-Ayanz 2017). Only species probability maps are available, which is a different matter with respect to their actual presence. Another aspect that adds error was the resampling that was required to standardize and process the maps at the same spatial resolution (100 m), often being the case of resampling from a higher spatial resolution (*e.g.*, 10 or 30 m) to the final resolution of 100 m for both CBH and CBD rasters. A last note can be related to land-cover change, that can play a key role in wrong attribution of CBH and CBD values were tree cover is not present anymore or has reduced canopy density (Akbar Hossain, Masiero, and Pirotti 2022).

The high uncertainty of CBD was expected as it aggregates uncertainties from estimations of the multiple factors that were used to calculate the final CBD values. It should be kept in mind that the input variables, each with its own estimated error, included canopy height, which was used to infer stem diameter, which was in turn used to infer foliage fraction. Each step implicates a degree of uncertainty, which adds up through the well-known chain rule. In particular, it should be noted that the functions to estimate the foliage fraction from DBH are such that small errors in DBH already cascade to large changes in fraction values. Nevertheless, the CBD map will provide a more probable value at that specific location. In addition, uncertainties to predict CBD are also produced by the biomass estimation at continental scales, where some authors, such as Huang et al. (2015) and Avitabile and Camia (2018), mentioned that at large continental

scales some discrepancies arise at pixel levels, where aboveground forest biomass can be underestimated or overestimated depending on the different inputs and modeling approaches used (Avitabile and Camia 2018), producing additional uncertainty for CBD estimations.

From the results shown in Figure 7, we can also assume that the pan-European map can be used with higher reliability when aggregated over larger areas, which is the objective of this work. The provided maps are meant to provide a regional-scale perspective of the spatial distribution of canopy fuels. The provided information will help to plan actions and interventions that aim at mitigating fire impacts. In particular, considering that climate change scenarios will change the temporal and spatial distribution of aridity and thus change the dynamics of fire hazards.

6. Conclusions

This work reports on the estimation of two important forest canopy fuel parameters, canopy base height (CBH) and canopy bulk density (CBD). The estimation was carried out using Earth observation data that was processed by a mixed approach that uses artificial intelligence and allometric models. Allometric models were defined specifically for this study using a combination of open data and ad-hoc contributions from coauthors. CBH and CBD maps at the European scale for the year 2020 at an approximate resolution of 100 m and with respective uncertainties are provided as the final product and to be used an operational scale, comparing to previous coarse maps (1 km). These two layers of information are

fundamental inputs for further modeling the behavior of wildfires and extreme wildfire events. Validation was provided through an independent dataset of 804 sample plots. The specific metrics reported CBH and CBD having respectively the following accuracies: (i) coefficient of correlation R of 0.445 and 0.330 (p-value < 0.001); (ii) root mean square of errors (RMSE) of 3.9 m and 0.099 kg m^{-3}; and (iii) a mean absolute percentage error (MAPE) of 61% and 76%. Regarding CBD, the accuracy metrics improved significantly if considering only cells covered by 80% or more forest canopy, to $R = 0.457$, RMSE = 0.085, and MAPE = 59%. This degree of accuracy was adequate and expected, as ground samples might not be representative of the forest variability in the 100 m raster cell, and models naturally propagate uncertainty. We can therefore assume with a reasonable degree of significance that the resulting maps can support planning and mitigation efforts in addressing fire-related actions.

Acknowledgments

Disclosure statement

No potential conflict of interest was reported by the author(s).

Funding

Notes on contributors

Erico Kutchartt received his degree in Forest Engineering from Universidad Austral de Chile in 2013, Master in European Forestry from Mendel University in Brno in 2017, and the PhD in Land Environment Resources and Health Program from University of Padova in 2022. He is currently a Post-Doctoral Fellow at the Forest Science and Technology Centre of Catalonia and at the University of Padova, focusing on the application of remote sensing, laser scanning, and photogrammetry in forestry.

José Ramón González Olabarria received his degree in Technical Agricultural Engineering from the Public University of Navarra in 1998, Forest Engineering from the University of Lleida in 2001, Master of Forest Science from the University of Joensuu (Finland) in 2002, and PhD in Forest Sciences also from the University of Joensuu in 2006. He is currently a senior researcher at the Forest Science and Technology Centre of Catalonia (CTFC), specialising in forest planning, forest fires, and ecosystem services.

Antoni Trasobares received his degree in Technical Agricultural Engineering from the Universitat Politècnica de Catalunya (1996) and the degree in Forest Engineering from the University of Lleida in 1998, Master of Forest Science from the University of Joensuu (Finland) in 1999, and PhD in Forest Management and Economy also from the University of Joensuu in 2004. He was the former General Director of Natural Environment and Biodiversity at Generalitat de Catalunya (2013 – 2016) and he is the current General Director of CTFC and coordinator of the FIRE-RES H2020 project.

Núria Aquilué received her BSc in Mathematics from the Universitat Politècnica de Catalunya (Spain) in 2005, MSc in Remote Sensing and Geographic Information Systems from Universitat Autònoma de Barcelona (Spain) in 2010, and the PhD in Environmental Sciences from Université du Québec à Montréal (Canada) in 2018. She is currently a Juan de la Cierva Post-Doctoral fellow at the Forest Science and Technology Centre of Catalonia (Spain) and associated researcher at Centre d'Étude de la Forêt (Canada), focusing on the development and application of forest models and spatial optimization methods to design resilient agroforest landscapes.

Juan Guerra Hernández obtained his degree in Forest Engineering from University of Córdoba (UCO) (Spain) in 2005, MSc in Biology and Vegetable Production from University of Extremadura (Spain) in 2010 and the PhD in Forestry and Natural Resources from University of Lisbon in 2018. He is currently a CEEC Research position at Forest Research Centre (CEF) of University of Lisbon, focusing on the application of remote sensing for forest monitoring and multiscale integration of different sources of information to support sustainable forest management.

Leónia Nunes received her degree in Forest Science Engineering from Coimbra College of Agriculture in 2003, Master in Forest engineering from University of Trás-os-Montes and Alto Douro in 2009, and the PhD in Forestry Sciences from University of Trás-os-Montes and Alto Douro in 2014. She is currently a researcher at the Centre for Applied Ecology Prof. Baeta Neves (CEABN-InBIO) from The School of Agriculture, University of Lisbon (ISA/ULisboa), focusing on the spatial structure of forest, modelling the growth of ecosystems, National Forest Inventories and recently she has been collaborating with municipalities in the estimation of urban environmental benefits.

Ana Catarina Sequeira received her degree and MSc in Landscape Architecture from The School of Agriculture, University of Lisbon (ISA/ULisboa), and a Ph.D. in Geography from the Complutense University of Madrid in 2020. She is currently a researcher at the Centre for Applied Ecology Prof. Baeta Neves (CEABN-InBIO) from The School of Agriculture, University of Lisbon (ISA/ULisboa), focusing on wildfire prevention, geospatial planning, and fire-smart landscapes and communities.

Brigite Botequim earned her Ph.D. in Forestry and Natural Resources from the University of Lisbon (ISA/ULisboa) (2015), complemented by an MSc in Statistics and Information Management from ULisboa (2008), and a BSc in Forest Engineering from ESACB, Instituto Politécnico de Castelo Branco (2002). She leads initiatives for fire-resilient territories in Europe. As a Senior Researcher, she focuses on a cohesive approach to address rural fire challenges within forest ecosystem management. Actively contributing to wildfire tools and ecosystem service assessments.

Marius Hauglin received his M.Sc. in forestry from the Norwegian University of Life Sciences in 2007, and Ph.D. in forest mensuration from the Norwegian University of Life Sciences in 2012. He is since 2018 a researcher at the National Forest Inventory at the Norwegian Institute of Bioeconomy Research. His main research is in forest resource mapping using remote sensing.

Palaiologos Palaiologou is a Geographer with a MSc in "Geography and Applied Geo-Informatics" and a PhD in Geography of Natural Disasters from the Department of Geography, University of the Aegean, Greece. During 2016-2018, he lived in the USA, working on wildfire risk, effects, and behaviour research as a visiting scholar for the International Visitor Program of the USDA Forest Service, in collaboration with Portland State University and Oregon State University. Currently, he is an Assistant Professor at the Agricultural University of Athens, Department of Forestry and Natural Environment Management, in the field of Forest Protection.

Adrian Cardil received his PhD with honours in Fire Science at the University of Lleida (Spain) in 2015 and was Awarded by the International Association of Wildland Fire (Early Career Research Award, 2022). He has carried out research in international research groups abroad on fire modelling, weather and ecology, establishing a broad network of international collaborators.

Martino Rogai received his master degree in "Forestry and Environmental Sciences" at the University of Florence, Italy in 2015, his bachelor degree in 2012. He is currently working at National Research Council (CNR) of Italy and attending his PhD in "Forestry and Environmental Management" at the University of Lleida, Spain, focusing on wildfires, remote sensing, preventive silviculture, and forestry mechanisation.

Vassil Vassilev received his MSc degree in Ecology from the Biological Faculty of the Sofia University, Bulgaria in 2000. He is currently a PhD student in the Space Research and Technology Institute of the Bulgarian Academy of Science, focusing on application of remote sensing data and AI in dynamic fuel model research.

François Pimont is a senior scientist who received his PhD in Environmental Sciences from University of Marseille in 2008. He is the head of the Fire Physics and Ecology Team in the Mediterranean Forest Research Unit (URFM) of INRAE in Avignon. He focuses on fire behavior and fire activity modelling, fuel modelling and mapping and climate change effects.

Olivier Martin-Ducup received his PhD in Forest ecology from Université du Quebec à Montreal (UQAM) in Canada in 2017. He is generally working on three-dimensional characterization of vegetation structure using LiDAR data (TLS, MLS, ULS, and ALS). He is currently working as a Post-Doctoral fellow at the French institute for agronomy and environment (INRAE) in the laboratory of research of Mediterranean ecosystem (URFM) in Avignon for characterising and mapping fuel for forest fire hazard assessment from air-borne ALS data.

Francesco Pirotti received his Major in Forestry and Environmental Sciences from the University of Padova in 2002 and his PhD in the Land Environment Resources and Health Program also from the University of Padova in 2005. He is currently associate professor at the University of Padova, teaching courses on spatial data analysis, surveying, and remote sensing. His research is oriented towards the application of remote sensing to the environmental sciences.

ORCID

Erico Kutchartt http://orcid.org/0000-0002-9134-4591
José Ramón González-Olabarria http://orcid.org/0000-0002-5040-712X
Antoni Trasobares http://orcid.org/0000-0002-8123-9405
Núria Aquilué http://orcid.org/0000-0001-7911-3144
Juan Guerra-Hernández http://orcid.org/0000-0003-3518-2978
Leónia Nunes http://orcid.org/0000-0002-2617-0468
Ana Catarina Sequeira http://orcid.org/0000-0002-5269-0643
Brigite Botequim http://orcid.org/0000-0002-6661-190X
Marius Hauglin http://orcid.org/0000-0003-2230-1288
Palaiologos Palaiologou http://orcid.org/0000-0001-8507-5201

Adrian Cardil http://orcid.org/0000-0002-0185-3959
Martino Rogai http://orcid.org/0009-0001-2977-2931
Vassil Vassilev http://orcid.org/0000-0003-3141-9456
Francois Pimont http://orcid.org/0000-0002-9842-6207
Olivier Martin-Ducup http://orcid.org/0000-0003-3795-1611
Francesco Pirotti http://orcid.org/0000-0002-4796-6406

Data availability statement

References

Akbar Hossain, K., M. Masiero, and F. Pirotti. 2022. "Land Cover Change Across 45 Years in the world's Largest Mangrove Forest (Sundarbans): The Contribution of Remote Sensing in Forest Monitoring." *European Journal of Remote Sensing* 1–17. https://doi.org/10.1080/22797254.2022.2097450.

Alberdi, I., R. Michalak, C. Fischer, P. Gasparini, U. B. Brändli, S. M. Tomter, A. Kuliesis, et al. 2016. "Towards Harmonized Assessment of European Forest Availability for Woody Supply in Europe." *Forest Policy and Economics* 70:20–29. https://doi.org/10.1016/j.forpol.2016.05.014.

Alberdi, I., R. Vallejo, J. G. Álvarez-González, S. Condés, E. González-Ferreiro, S. Guerrero, L. Hernández, et al. 2017. "The Multi-Objective Spanish National Forest Inventory." *Forest Systems* 26 (2): e04S. https://doi.org/10.5424/fs/2017262-10577.

Alexander, M. E., and M. G. Cruz. 2011. "Interdependencies Between Flame Length and Fireline Intensity in Predicting Crown Fire Initiation and Crown Scorch Height." *International Journal of Wildland Fire* 21 (2): 95–113. https://doi.org/10.1071/WF11001.

Andersen, H. E., R. J. McGaughey, and S. E. Reutebuch. 2005. "Estimating Forest Canopy Fuel Parameters Using LIDAR Data." *Remote Sensing of Environment* 94 (4): 441–449. https://doi.org/10.1016/j.rse.2004.10.013.

Aragoneses, E., M. García, P. Ruiz-Benito, and E. Chuvieco. 2024. "Mapping Forest Canopy Fuel Parameters at European Scale Using Spaceborne LiDAR and Satellite Data." *Remote Sensing of Environment* 303:114005. https://doi.org/10.1016/j.rse.2024.114005.

Aragoneses, E., M. García, M. Salis, L. M. Ribeiro, and E. Chuvieco. 2023. "Classification and Mapping of European Fuels Using a Hierarchical, Multipurpose Fuel Classification System." *Earth System Science Data* 15 (3): 1287–1315. https://doi.org/10.5194/essd-15-1287-2023.

Arellano-Pérez, S., F. Castedo-Dorado, C. A. López-Sánchez, E. González-Ferreiro, Z. Yang, R. A. Díaz-Varela, J. G. Alvárez-González, J. A. Vega, and A. D. Ruiz-González. 2018. "Potential of Sentinel-2A Data to Model Surface and Canopy Fuel Characteristics in Relation to Crown Fire Hazard." *Remote Sensing* 10 (10): 1645. https://doi.org/10.3390/rs10101645.

Arkin, J., N. C. Coops, L. D. Daniels, and A. Plowright. 2023. "Canopy and Surface Fuel Estimations Using RPAS and Ground-Based Point Clouds." *Forestry: An International Journal of Forest Research* cpad020:1–14. https://doi.org/10.1093/forestry/cpad020.

Aussenac, R., J. M. Monnet, M. Klopčič, P. Hawrylo, J. Socha, M. Mahnken, M. Gutsch, T. Cordonnier, and P. Vallet. 2023. "Diameter, Height and Species of 42 Million Trees in Three European Landscapes Generated from Field Data and Airborne Laser Scanning Data." *Open Research Europe* 3:32. https://doi.org/10.12688/openreseurope.15373.2.

Avitabile, V., and A. Camia. 2018. "An Assessment of Forest Biomass Maps in Europe Using Harmonized National Statistics and Inventory Plots." *Forest Ecology & Management* 409:489–498. https://doi.org/10.1016/j.foreco.2017.11.047.

Bonannella, C., T. Hengl, J. Heisig, L. Parente, M. N. Wright, M. Herold, and S. de Bruin. 2022. "Forest Tree Species Distribution for Europe 2000-2020: Mapping Potential and Realized Distributions Using Spatiotemporal Machine Learning." *PeerJ* 10:e13728. https://doi.org/10.7717/peerj.13728.

Botequim, B., P. M. Fernandes, J. G. Borges, E. González-Ferreiro, and J. Guerra-Hernández. 2019. "Improving Silvicultural Practices for Mediterranean Forests Through Fire Behaviour Modelling Using LiDAR-Derived Canopy Fuel Characteristics." *International Journal of Wildland Fire* 28 (11): 823–839. https://doi.org/10.1071/WF19001.

Bowman, D. M. J. S., G. J. Williamson, J. T. Abatzoglou, C. A. Kolden, M. A. Cochrane, and A. M. S. Smith. 2017. "Human Exposure and Sensitivity to Globally Extreme Wildfire Events." *Nature Ecology & Evolution* 1 (3): 0058. https://doi.org/10.1038/s41559-016-0058.

Breidenbach, J., and R. Astrup. 2012. "Small Area Estimation of Forest Attributes in the Norwegian National Forest Inventory." *European Journal of Forest Research* 131 (4): 1255–1267. https://doi.org/10.1007/s10342-012-0596-7.

Cardil, A., G. M. Delegu, and D. M. Molina-Terrén. 2017. "Fatalities in Wildland Fires from 1945 to 2015 in Sardinia (Italy)." *Cerne* 23 (2): 175–184. https://doi.org/10.1590/01047760201723022266.

Chamberlain, C. P., A. J. Sánchez Meador, and A. E. Thode. 2021. "Airborne Lidar Provides Reliable Estimates of Canopy Base Height and Canopy Bulk Density in Southwestern Ponderosa Pine Forests." *Forest Ecology & Management* 481:118695. https://doi.org/10.1016/j.foreco.2020.118695.

Chuvieco, E., M. Yebra, S. Martino, K. Thonicke, M. Gómez-Giménez, J. San-Miguel, D. Oom, et al. 2023. "Towards an Integrated Approach to Wildfire Risk Assessment: When, Where, What, and How May the Landscapes Burn." *Fire* 6 (5): 215. https://doi.org/10.3390/fire6050215.

Cruz, M. G., M. E. Alexander, and R. H. Wakimoto. 2003. "Assessing Canopy Fuel Stratum Characteristics in Crown Fire Prone Fuel Types of Western North

America." *International Journal of Wildland Fire* 12 (1): 39–50. https://doi.org/10.1071/WF02024.

Diakakis, M., G. Xanthopoulos, and L. Gregos. 2016. "Analysis of Forest Fire Fatalities in Greece: 1977–2013." *International Journal of Wildland Fire* 25 (7): 797–809. https://doi.org/10.1071/WF15198.

Dubayah, R., J. B. Blair, S. Goetz, L. Fatoyinbo, M. Hansen, S. Healey, M. Hofton, et al. 2020. "The Global Ecosystem Dynamics Investigation: High-Resolution Laser Ranging of the Earth's Forests and Topography." *Science of Remote Sensing* 1:100002. https://doi.org/10.1016/j.srs.2020.100002.

Eid, T., T. Gobakken, and E. Næsset. 2004. "Comparing Stand Inventories for Large Areas Based on Photo-Interpretation and Laser Scanning by Means of Cost-Plus-Loss Analyses." *Scandinavian Journal of Forest Research* 19 (6): 512–523. https://doi.org/10.1080/02827580410019463.

El Garroussi, S., F. Di Giuseppe, C. Barnard, and F. Wetterhall. 2024. "Europe Faces Up to Tenfold Increase in Extreme Fires in a Warming Climate." *Npj Climate and Atmospheric Science* 7 (1): 30. https://doi.org/10.1038/s41612-024-00575-8.

Engelstad, P. D., M. Falkowski, P. Wolter, A. Poznanovic, and P. Johnson. 2019. "Estimating Canopy Fuel Attributes from Low-Density LiDAR." *Fire* 2 (3): 38. https://doi.org/10.3390/fire2030038.

Erdody, T. L., and L. M. Moskal. 2010. "Fusion of LiDAR and Imagery for Estimating Forest Canopy Fuels." *Remote Sensing of Environment* 114 (4): 725–737. https://doi.org/10.1016/j.rse.2009.11.002.

Ex, S. A., F. W. Smith, T. L. Keyser, and S. A. Rebain. 2016. "Estimating Canopy Bulk Density and Canopy Base Height for Interior Western US Conifers Stands." *Forest Science* 62 (6): 690–697. https://doi.org/10.5849/forsci.15-118.

Fick, S., and R. Hijmans. 2017. "WorldClim 2: New 1-Km Spatial Resolution Climate Surfaces for Global Land Areas." *International Journal of Climatology* 37 (12): 4302–4315. https://doi.org/10.1002/joc.5086.

Finney, M. A. 2004. "FARSITE: Fire Area Simulator – Model Development and Evaluation." Research paper RMRS-R-4 Revised, 47. USDA United States Department of Agriculture, Forest Service. Rocky Mountain Research Station.

Finney, M. A. 2006. "An Overview of FlamMap Fire Modelling Capabilities." USDA Forest Service Proceedings RMRS-P-41, 213–220. Fort Collins, CO. U. S Department of Agriculture, Forest Service, Rocky Mountain Research Station.

Finney, M. A., and T. P. Grumstrup. 2023. "Effect of Flame Zone Depth on the Correlation of Flame Length with Fireline Intensity." *International Journal of Wildland Fire* 32 (7): 1135–1147. https://doi.org/10.1071/WF22096.

Finney, M. A., C. W. McHugh, I. C. Grenfell, K. L. Riley, and K. C. Short. 2011. "A Simulation of Probabilistic Wildfire Risk Components for the Continental United States." *Stochastic Environmental Research and Risk Assessment* 25 (7): 973–1000. https://doi.org/10.1007/s00477-011-0462-z.

Forrester, D. I., A. Benneter, O. Bouriaud, and J. Bauhaus. 2017a. "Diversity and Competition Influence Tree Allometric Relationships – Developing Functions for Mixed-Species Forests." *The Journal of Ecology* 105 (3): 761–774. https://doi.org/10.1111/1365-2745.12704.

Forrester, D. I., I. H. H. Tachauer, P. Annighoefer, I. Barbeito, H. Pretzsch, R. Ruiz-Peinado, H. Stark, et al. 2017b. "Generalized Biomass and Leaf Area Allometric Equations for European Tree Species Incorporating Stand Structure, Tree Age and Climate." *Forest Ecology & Management* 396:160–175. https://doi.org/10.1016/j.foreco.2017.04.011.

Fridman, J., S. Holm, M. Nilsson, P. Nilsson, A. H. Ringvall, and G. Ståhl. 2014. "Adapting National Forest Inventories to Changing Requirements - the Case of the Swedish National Forest Inventory at the Turn of the 20th Century." *Silva Fennica* 48 (3): 1095. https://doi.org/10.14214/sf.1095.

Ganteaume, A., A. Camia, M. Jappiot, J. San-Miguel-Ayanz, M. Long-Fournel, and C. Lampin. 2013. "A Review of the Main Driving Factors of Forest Fire Ignition Over Europe." *Environmental Management* 51 (3): 651–662. https://doi.org/10.1007/s00267-012-9961-z.

García-Llamas, P., S. Suárez-Seoane, A. Taboada, A. Fernández-Manso, C. Quintano, V. Fernández-García, J. M. Fernández-Guisuraga, E. Marcos, and L. Calvo. 2019. "Environmental Drivers of Fire Severity in Extreme Fire Events That Affect Mediterranean Pine Forest Ecosystems." *Forest Ecology & Management* 15:24–32. https://doi.org/10.1016/j.foreco.2018.10.051.

Gasparini, P., L. Di Cosmo, A. Floris, and D. De Laurentis. 2022. *Italian National Forest Inventory – Methods and Results of the Third Survey*, 576. Springer Tracts in Civil Engineering. Springer Cham. https://doi.org/10.1007/978-3-030-98678-0.

Gobakken, T., and E. Næsset. 2008. "Assessing Effects of Laser Point Density, Ground Sampling Intensity, and Field Sample Plot Size on Biophysical Stand Properties Derived from Airborne Laser Scanner Data." *Canadian Journal of Forest Research* 38 (5): 1095–1109. https://doi.org/10.1139/X07-219.

González-Olabarria, J. R., J. Carrasco, C. Pais, J. Garcia-Gonzalo, D. Palacios-Meneses, R. Mahaluf-Recasens, O. Porkhum, and A. Weintraub. 2023. "A Fire Spread Simulator to Support Tactical Management Decisions for Mediterranean Landscapes." *Frontiers in Forests and Global Change* 6:1071484. https://doi.org/10.3389/ffgc.2023.1071484.

González-Olabarria, J. R., F. Rodríguez, A. Fernández-Landa, and B. Mola-Yudego. 2012. "Mapping Fire Risk in the Model Forest of Urbión (Spain) Based on Airborne LiDAR Measurements." *Forest Ecology & Management* 282:149–156. https://doi.org/10.1016/j.foreco.2012.06.056.

Gorelick, N., M. Hancher, M. Dixon, S. Ilyushchenko, D. Thau, and R. Moore. 2017. "Google Earth Engine: Planetary-Scale Geospatial Analysis for Everyone." *Remote Sensing of Environment* 202:18–27. https://doi.org/10.1016/j.rse.2017.06.031.

Grüning, M., R. Seidl, and C. Senf. 2023. "Increasing Aridity Causes Larger and More Severe Forest Fires Across Europe." *Global Change Biology* 29 (6): 1648–1659. https://doi.org/10.1111/gcb.16547.

Gschwantner, T., I. Alberdi, S. Bauwens, S. Bender, D. Borota, M. Bosela, O. Bouriaud, et al. 2022. "Growing Stock Monitoring by European National Forest Inventories: Historical Origins, Current Methods and Harmonisation." *Forest Ecology & Management* 505:119869. https://doi.org/10.1016/j.foreco.2021.119868.

H2O.ai. 2022. "h2o: R Interface for H2O. R Package Version 3.42.0.2."

Hansen, M. C., P. V. Potapov, R. Moore, M. Hancher, S. A. Turubanova, A. Tyukavina, D. Thau, et al. 2013. "High-Resolution Global Maps of 21st-century Forest Cover Change." *Science* 342 (6160): 850–853. https://doi.org/10.1126/science.1244693.

Hauck, W. W., and S. Anderson. 1984. "A Survey Regarding the Reporting of Simulation Studies." *American Statistician* 38 (3): 214–216. https://doi.org/10.1080/00031305.1984.10483206.

Hemmerling, J., D. Pflugmacher, and P. Hostert. 2021. "Mapping Temperate Forest Tree Species Using Dense Sentinel-2 Time Series." *Remote Sensing of Environment* 267:112743. https://doi.org/10.1016/j.rse.2021.112743.

Hijmans, R. J., S. E. Cameron, J. L. Parra, P. G. Jones, and A. Jarvis. 2005. "Very High Resolution Interpolated Climate Surfaces for Global Land Areas." *International Journal of Climatology* 25 (15): 1965–1978. https://doi.org/10.1002/joc.1276 .

Hoffrén, R., M. T. Lamelas, J. de la Riva, D. Domingo, A. L. Montealegre, A. García-Martín, and S. Revilla. 2023. "Assessing GEDI-NASA System for Forest Fuels Classification Using Machine Learning Techniques." *International Journal of Applied Earth Observation and Geoinformation* 116:103175. https://doi.org/10.1016/j.jag.2022.103175.

Hsieh, P. F., L. C. Lee, and N. Y. Chen. 2001. "Effect of Spatial Resolution on Classification Errors of Pure and Mixed Pixels in Remote Sensing." *IEEE Transactions on Geoscience & Remote Sensing* 39 (12): 2657–2663. https://doi.org/10.1109/36.975000.

Huang, W., A. Swatantra, K. Johnson, L. Duncanson, H. Tang, J. O. Dunne, G. Hurtt, et al. 2015. "Local Discrepancias in Continental Scale Biomass Maps: A Case Study Over Forested and Non-Forested Landscapes in Maryland, USA." *Carbon and Balance Management* 10 (1): 19. https://doi.org/10.1186/s13021-015-0030-9.

Jones, M. W., J. T. Abatzoglou, S. Veraverbeke, N. Andela, G. Lasslop, M. Forkel, A. J. P. Smith, et al. 2022. "Global and Regional Trends and Drivers of Fire Under Climate Change." *Reviews of Geophysics* 60 (3): c2020RG000726. https://doi.org/10.1029/2020RG000726.

Kalogiannidis, S., F. Chatzitheodoridis, D. Kalfas, C. Patitsa, and A. Papagrigoriou. 2023. "Socio-Psychological, Economic and Environmental Effects of Forest Fires." *Fire* 6 (7): 280. https://doi.org/10.3390/fire6070280.

Krsnik, G., E. Busquets Olivé, M. Piqué Nicolau, A. Larrañaga, A. Cardil, J. García-Gonzalo, and J. R. González Olabarria. 2020. "Regional Level Data Server for Fire Hazard Evaluation and Fuel Treatments Planning." *Remote Sensing* 12 (24): 4124. https://doi.org/10.3390/rs12244124.

Kudláčková, L., M. Poděbradská, M. Bláhová, E. Cienciala, J. Beranová, C. McHugh, M. Finney, et al. 2023. "Using FlamMap to Assess Wildfire Behavior in Bohemian Switzerland National Park." *Natural Hazards* 120 (4): 3943–3977. https://doi.org/10.1007/s11069-023-06361-8.

Kutchartt, E., J. Gayoso, F. Pirotti, Á. Bucarey, J. Guerra, J. Hernández, P. Corvalán, K. Drápela, M. Olson, and M. Zwanzig. 2021. "Aboveground Tree Biomass of *Araucaria Araucana* in Southern Chile: Measurements and Multi-Objective Optimization of Biomass Models." *iForest – Biogeosciences and Forestry* 14 (1): 61–70. https://doi.org/10.3832/ifor3492-013.

Kutchartt, E., M. Pedron, and F. Pirotti. 2022. "Assessment of Canopy and Ground Height Accuracy from GEDI LiDAR Over Steep Mountain Areas." *ISPRS Annals of the Photogrammetry, Remote Sensing & Spatial Information Sciences* 3-2022:431–438. https://doi.org/10.5194/isprs-annals-V-3-2022-431-2022.

Lang, N., W. Jetz, K. Schindler, and J. D. Wegner. 2023. "A High-Resolution Canopy Height Model of the Earth." *Nature Ecology & Evolution* 7 (11): 1778–1789. https://doi.org/10.1038/s41559-023-02206-6.

Latty, R. S., R. Nelson, B. Markham, D. Williams, and D. Toll. 1985. "Performance Comparisons Between Information Extraction Techniques Using Variable Spatial Resolution Data." *Photogrammetric Engineering & Remote Sensing* 51. 0099–1112. NASA Technical Reports Server.

Lozano, O. M., M. Salis, A. A. Ager, B. Arca, F. J. Alcasena, A. T. Monteiro, M. A. Finney, et al. 2016. "Assessing Climate Change Impacts on Wildfire Exposure in Mediterranean Areas." *Risk Analysis* 31 (10): 1898–1916. https://doi.org/10.1111/risa.12739.

Main, R., M. A. Cho, R. Mathieu, M. M. O'Kennedy, A. Ramoelo, and S. Koch. 2011. "An Investigation into Robust Spectral Indices for Leaf Chlorophyll Estimation." *Isprs Journal of Photogrammetry & Remote Sensing* 66 (6): 751–761. https://doi.org/10.1016/j.isprsjprs.2011.08.001.

Maltamo, M., T. Karjalainen, J. Repola, and J. Vauhkonen. 2018. "Incorporating Tree- and Stand- Level Information on Crown Base Height into Multivariate Forest Management Inventories Based on Airborne Laser Scanning." *Silva Fennica* 52 (3): 10006. https://doi.org/10.14214/sf.10006.

Maltamo, M., J. Räty, L. Korhonen, E. Kotivuori, M. Kukkonen, H. Peltola, J. Kangas, et al. 2020. "Prediction of Forest Canopy Fuel Parameters in Managed Boreal Forests Using Multispectral and Unispectral Airborne Laser Scanning Data and Aerial Images." *European Journal of Remote Sensing* 53 (1): 245–257. https://doi.org/10.1080/22797254.2020.1816142.

Marino, E., J. L. Tomé, C. Hernando, M. Guijarro, and J. Madrigal. 2022. "Transferability of Airborne LiDAR Data for Canopy Fuel Mapping: Effect of Pulse Density and Model Formulation." *Fire* 5 (5): 126. https://doi.org/10.3390/fire5050126.

Mauri, A., G. Strona, and J. San-Miguel-Ayanz. 2017. "EU-Forest, a High-Resolution Tree Occurrence Dataset for Europe." *Scientific Data* 4 (1): 160123. https://doi.org/10.1038/sdata.2016.123.

Mihajlovski, B., P. M. Fernandes, J. M. Pereira, and J. Guerra-Hernández. 2023. "Comparing Forest

Understory Fuel Classification in Portugal Using Discrete Airborne Laser Scanning Data and Satellite Multi-Source Remote Sensing Data." *Fire* 6 (9): 327. https://doi.org/10.3390/fire6090327.

Miller, H. R. 2011. *Optimization: Foundations and Applications*. New York, NY USA: John Wiley & Sons.

Molina-Terrén, D. M., G. Xanthopoulos, M. Diakakis, L. Ribeiro, D. Caballero, G. M. Delogu, D. X. Viegas, et al. 2019. "Analysis of Forest Fire Fatalities in Southern Europe: Spain, Portugal, Greece and Sardinia (Italy)." *International Journal of Wildland Fire* 28 (2): 85–98. https://doi.org/10.1071/WF18004.

Monedero, S., J. Ramirez, and A. Cardil. 2019. "Predicting Fire Spread and Behaviour on the Fireline. Wildfire Analyst Pocket: A Mobile App for Wildland Fire Prediction." *Ecological Modelling* 392:103–107. https://doi.org/10.1016/j.ecolmodel.2018.11.016.

Moran, C. J., V. R. Kane, and C. A. Seielstad. 2020. "Mapping Forest Canopy Fuels in the Western United States with LiDAR-Landsat Covariance." *Remote Sensing* 12 (6): 1000. https://doi.org/10.3390/rs12061000.

Or, D., E. Furtak-Cole, M. Berli, R. Shillito, H. Ebrahimian, H. Vahdat-Aboueshagh, and S. A. McKenna. 2023. "Review of Wildfire Modeling Considering Effects on Land Surfaces." *Earth-Science Reviews* 245:104569. https://doi.org/10.1016/j.earscirev.2023.104569.

Pirotti, F., O. Adedipe, and B. Leblon. 2023a. "Sentinel-1 Response to Canopy Moisture in Mediterranean Forests Before and After Fire Events." *Remote Sensing* 15 (3): 823. Articolo 3. https://doi.org/10.3390/rs15030823.

Pirotti, F., J. R. González-Olabarria, and E. Kutchartt. 2023b. "Updating Aboveground Biomass at a Pan-European Scale Through Satellite Data and Artificial Intelligence." *International Archives of the Photogrammetry, Remote Sensing and Spatial Information Sciences* XLVIII-1/W2-2023:1763–1769. https://doi.org/10.5194/isprs-archives-XLVIII-1-W2-2023-1763-2023.

Pison, G., S. Van Aelst, and G. Willems. 2002. "Small Sample Corrections for LTS and MCD." *Metrika* 55 (1–2): 111–123. https://doi.org/10.1007/s001840200191.

Pittman, R. C., and B. Hu. 2023. "Contribution of Topographic Features and Categorization Uncertainty for a Tree Species Classification in the Boreal Biome of Northern Ontario." *GIScience & Remote Sensing* 60 (1): 2214994. https://doi.org/10.1080/15481603.2023.2214994.

Portsmouth, A., Ü. Niinemets, L. Truus, and M. Pensa. 2005. "Biomass Allocation and Growth Rates in *Pinus Sylvestris* are Interactively Modified by Nitrogen and Phosphorus Availabilities and by Tree Size and Age." *Canadian Journal of Forest Research* 35 (10): 2346–2359. https://doi.org/10.1139/x05-155.

Potapov, P., X. Li, A. Hernandez-Serna, A. Tyukavina, M. C. Hansen, A. Kommareddy, A. Pickens, et al. 2021. "Mapping Global Forest Canopy Height Through Integration of GEDI and Landsat Data." *Remote Sensing of Environment* 253:112165. https://doi.org/10.1016/j.rse.2020.112165.

Pucher, C., M. Neumann, and H. Hasenauer. 2022. "An Improved Forest Structure Data Set for Europe." *Remote Sensing* 14 (2): 395. https://doi.org/10.3390/rs14020395.

Rocha, K. D., C. A. Silva, D. N. Cosenza, M. Mohan, C. Klauberg, M. B. Schlickmann, J. Xia, et al. 2023. "Crown-Level Structure and Fuel Load Characterization from Airborne and Terrestrial Laser Scanning in a Longleaf Pine (*Pinus Palustris* Mill.) Forest Ecosystem." *Remote Sensing* 15 (4): 1002. https://doi.org/10.3390/rs15041002.

Rodríguez, F., M. G. Guzmán, J. M. Olmo, E. J. Carmona, J. R. M. Martínez, C. Hernando, R. V. Muñoz, J. A. V. Hidalgo, and others. 2017. "Assessment of Crown Fire Initiation and Spread Models in Mediterranean Conifer Forests by Using Data from Field and Laboratory Experiments." *Forest Systems* 26 (2): 12. https://doi.org/10.5424/fs/2017262-10652.

Rollins, M. G. 2009. "LANDFIRE: A Nationally Consistent Vegetation, Wildland Fire, and Fuel Assessment." *International Journal of Wildland Fire* 18 (3): 235–249. https://doi.org/10.1071/WF08088.

Rothermel, R. C. 1983. *How to Predict the Spread and Intensity of Forest and Range Fires*, 161. Ogden, UT, USA: USDA Forest Service, Intermountain Forest and Range Experiment Station.

Rousseeuw, P. J. 1984. "Least Median of Squares Regression." *Journal of the American Statistical Association* 79 (388): 871–880. https://doi.org/10.1080/01621459.1984.10477105.

Ruffault, J., and F. Mouillot. 2017. "Contribution of Human and Biophysical Factors to the Spatial Distribution of Forest Fire Ignitions and Large Wildfires in a French Mediterranean Region." *International Journal of Wildland Fire* 26 (6): 498–508. https://doi.org/10.1071/WF16181.

Ruiz-González, A. D., and J. G. Álvarez-González. 2011. "Canopy Bulk Density and Canopy Base Height Equations for Assessing Crown Fire Hazard in *Pinus Radiata* Plantations." *Canadian Journal of Forest Research* 41 (4): 839–850. https://doi.org/10.1139/x10-237.

Saatchi, S., K. Halligan, D. G. Despain, and R. L. Crabtree. 2007. "Estimation of Forest Fuel Load from Radar Remote Sensing." *IEEE Transactions on Geoscience & Remote Sensing* 45 (6): 1726–1740. https://doi.org/10.1109/TGRS.2006.887002.

San-Miguel-Ayanz, J., T. Durrant, R. Boca, P. Maianti, G. Libertà, D. Oom, A. Branco, et al. 2023. *Advance Report on Forest Fires in Europe, Middle East and North Africa 2022*, 47. Luxembourg: Publications Office of the European Union. https://doi.org/10.2760/091540.

San-Miguel-Ayanz, J., J. M. Moreno, and A. Camia. 2013. "Analysis of Large Fires in European Mediterranean Landscapes: Lessons Learned and Perspectives." *Forest Ecology & Management* 294:11–22. https://doi.org/10.1016/j.foreco.2012.10.050.

Santoro, M., and O. Cartus. 2021. "ESA Biomass Climate Change Initiative (Biomass_cci): Global Datasets of Forest Above-Ground Biomass for the Years 2010, 2017 and 2018, V3." https://doi.org/10.5285/5F331C418E9F4935B8EB1B836F8A91B8.

Santoro, M., O. Cartus, U. Wegmüller, S. Besnard, N. Carvalhais, A. Araza, M. Herold, et al. 2022. "Global Estimation of Above-Ground Biomass from Spaceborne C-Band Scatterometer Observations Aided by LiDAR

Metrics of Vegetation Structure.” *Remote Sensing of Environment* 279:113114. https://doi.org/10.1016/j.rse.2022.113114.

Schindler, Z., T. Seifert, J. P. Sheppard, and C. Morhart. 2023. “Allometric Models for Above-Ground Biomass, Carbon and Nutrient Content of Wild Cherry (*Prunus Avium* L.) Trees in Agroforestry Systems.” *Annals of Forest Science* 80 (1): 28. https://doi.org/10.1186/s13595-023-01196-6.

Scott, J. H., and E. D. Reinhardt. 2001. “Assessing Crown Fire Potential by Linking Models of Surface and Crown Fire Behavior.” In *USDA Forest Service, Rocky Mountain Research Station*, 59. USA: Fort Collins, CO.

Shimada, M., T. Itoh, T. Motooka, M. Watanabe, T. Shiraishi, R. Thapa, and R. Lucas. 2014. “New Global Forest/non-Forest Maps from ALOS PALSAR Data (2007-2010).” *Remote Sensing of Environment* 155: 13–31. https://doi.org/10.1016/j.rse.2014.04.014.

Shin, P., T. Sankey, M. M. Moore, and A. E. Thode. 2018. “Evaluating Unmanned Aerial Vehicle Images for Estimating Forest Canopy Fuels in a Ponderosa Pine Stand.” *Remote Sensing* 10 (8): 1266. https://doi.org/10.3390/rs10081266.

Sileshi, G. W. 2014. “A Critical Review of Forest Biomass Estimation Models, Common Mistakes and Corrective Measures.” *Forest Ecology & Management* 329:237–254. https://doi.org/10.1016/j.foreco.2014.06.026.

Stefanidou, A., I. Z. Gitas, L. Korhonen, D. Stavrakoudis, and N. Georgopoulos. 2020. “LiDAR-Based Estimates of Canopy Base Height for a Dense Uneven-Aged Structured Forest.” *Remote Sensing* 12 (10): 1565. https://doi.org/10.3390/rs12101565.

Suarez-Gutierrez, L., W. A. Müller, and J. Marotzke. 2023. “Extreme Heat and Drought Typical of an End-Of-Century Climate Could Occur Over Europe Soon and Repeatedly.” *Communications Earth & Environment* 4 (1): 415. https://doi.org/10.1038/s43247-023-01075-y.

Tadono, T., H. Nagai, H. Ishida, F. Oda, S. Naito, K. Minakawa, and H. Iwamoto. 2016. “Generation of the 30 M-Mesh Global Digital Surface Model by ALOS PRISM.” *International Archives of the Photogrammetry, Remore Sensing and Spatial Information Sciences* B4: 157–162. https://doi.org/10.5194/isprs-archives-XLI-B4-157-2016.

Tedim, F., V. Leone, M. Amraoui, C. Bouillon, M. R. Coughlan, G. M. Delogu, P. M. Fernandes, et al. 2018. “Defining Extreme Wildfire Events: Difficulties, Challenges, and Impacts.” *Fire* 1 (1): 9. https://doi.org/10.3390/fire1010009.

Torabzadeh, H., R. Leiterer, A. Hueni, M. E. Schaepman, and F. Morsdorf. 2019. “Tree Species Classification in a Temperate Mixed Forest Using a Combination of Imaging Spectroscopy and Airborne Laser Scanning.” *Agricultural and Forest Meteorology* 279:107744. https://doi.org/10.1016/j.agrformet.2019.107744.

Turco, M., J. J. Rosa-Cánovas, J. Bedia, S. Jerez, J. P. Montávez, M. C. Llasat, and A. Provenzale. 2018. “Exacerbated Fires in Mediterranean Europe Due to Anthropogenic Warming Projected with Non-Stationary Climate-Fire Models.” *Nature Communications* 9 (1): 3821. https://doi.org/10.1038/s41467-018-06358-z.

Wagner, C. E. V. 1977. “Conditions for the Start and Spread of Crown Fine.” *Canadian Journal of Forest Research* 7 (1): 23–34. https://doi.org/10.1139/x77-004.

Wang, Y., X. Xi, C. Wang, X. Yang, P. Wang, S. Nie, and M. Du. 2022. “A Novel Method Based on Kernel Density for Estimating Crown Base Height Using UAV-Borne LiDAR Data.” *IEEE Geoscience & Remote Sensing Letters* 19:7004105. https://doi.org/10.1109/LGRS.2022.3171316.

Yurtgan, M., I. Baysal, and O. Küçük. 2022. “Fuel Characterization and Crown Fuel Load Prediction in Non-Treated Calabrian Pine (*Pinus Brutia* Ten.) Plantation Areas.” *iForest – Biogeosciences and Forestry* 15 (6): 458–464. https://doi.org/10.3832/ifor4048-015.

Zanaga, D., R. Van De Kerchove, W. De Keersmaecker, N. Souverijns, C. Brockmann, R. Quast, J. Wevers, et al. 2021. “ESA WorldCover 10 M 2020 v100.” https://doi.org/10.5281/ZENODO.5571936.

Appendix

Table S1. Species-specific allometric equations fitted to estimate the branch insertion height based on the total height as an explanatory variable for 16 tree species across Europe, including the metrics from the cross-validation using k-fold validation where k=20. β_0 (Intercept) is equal to zero. Figure S1 shows the plotted fitted models.

Species	N	β_1 (Slope)	R-squared (+SD)	RMSE (+SD)	MAPE (+SD)
Abies alba	304	0.253	0.802(0.0059)	2.039 (0.206)	11.1 (0.987)
Castanea sativa	4806	0.549	0.882(0.0007)	2.944 (0.377)	9.3 (1.121)
Corylus avellana	1685	0.637	0.923(0.0008)	2.143 (0.262)	9.2 (0.947)
Fagus sylvatica	5395	0.509	0.867(0.0004)	4.518 (0.906)	12.9 (2.388)
Olea europaea	594	0.628	0.946(0.0005)	1.119 (0.054)	7.3 (0.455)
Picea abies	11631	0.166	0.701(0.0009)	3.135 (0.048)	14.6 (0.084)
Pinus halepensis	6875	0.522	0.921(0.0004)	1.567 (0.033)	7.6 (0.165)
Pinus nigra	4878	0.501	0.927(0.0007)	1.745 (0.060)	7.8 (0.178)
Pinus pinea	1655	0.446	0.905(0.0009)	1.544 (0.077)	8.3 (0.287)
Pinus sylvestris	21913	0.468	0.909(0.0008)	2.254 (0.014)	8.0 (0.072)
Prunus avium	224	0.325	0.730(0.0052)	2.939 (0.336)	12.8 (0.728)
Quercus cerris	2244	0.409	0.905(0.0012)	1.359 (0.059)	7.6 (0.287)
Quercus ilex	18187	0.394	0.908(0.0004)	0.993 (0.014)	7.2 (0.072)
Quercus robur	4164	0.662	0.930(0.0012)	2.843 (0.085)	7.6 (0.301)
Quercus suber	479	0.352	0.913(0.0016)	1.653 (0.194)	8.3 (0.277)
Salix caprea	544	0.388	0.837(0.0047)	2.265 (0.149)	10.0 (0.726)

Table S2. Relationship to predict the diameter breast height based on total height using data from Aussenac et al. (2023) and from other projects for France, Poland, Slovenia and Italy. Results of the coefficient of determination are all significant with P-value < 0.001

Species	N	β_0	β_1	β_2	R-squared (+SD)	RMSE (+SD)	MAE (+SD)
Abies alba	1933156	1.3436	0.6874	0.0372	0.924 (0.0007)	4.9 (0.0260)	2.9 (0.0060)
Castanea sativa	141803	4.0980	-0.2394	0.0869	0.803 (0.00076)	7.1 (0.1880)	4.1 (0.0564)
Corylus avellana	87151	0.9046	0.5337	0.0365	0.981 (0.0005)	0.4 (0.0063)	0.3 (0.0033)
Fagus sylvatica	3401526	0.8648	0.3802	0.0470	0.891 (0.0005)	4.4 (0.0133)	2.7 (0.0034)
Olea europaea	353	-4.3107	3.1992	-0.0528	0.555 (0.1353)	4.7 (1.4807)	3.2 (0.7838)
Picea abies	2092487	1.3806	0.6790	0.0351	0.939 (0.0004)	3.8 (0.0157)	1.9 (0.0052)
Pinus halepensis	1992	-9.2907	3.3574	-0.0463	0.586 (0.0475)	6.8 (0.5510)	5.0 (0.2781)
Pinus nigra	5956	5.4561	1.1050	0.0119	0.621 (0.0345)	5.9 (0.2327)	4.5 (0.1842)
Pinus pinea	809	-2.3634	2.9791	-0.0297	0.569 (0.0914)	8.7 (1.3745)	6.2 (0.7248)
Pinus sylvestris	3149820	5.1299	-0.0554	0.0395	0.831 (0.0008)	4.0 (0.0112)	2.8 (0.0042)
Prunus avium	119316	-1.0741	0.5173	0.0574	0.774 (0.0037)	5.9 (0.0665)	3.6 (0.0318)
Quercus cerris	18972	0.6734	0.9954	0.0196	0.608 (0.0255)	5.4 (0.2986)	3.6 (0.0751)
Quercus ilex	12692	4.7826	0.4492	0.0679	0.510 (0.0502)	4.6 (0.4237)	3.0 (0.1072)
Quercus robur	313817	3.5610	0.1671	0.0461	0.897 (0.0019)	5.6 (0.0517)	3.2 (0.0210)
Quercus suber	2112	-2.5090	3.6174	0.0128	0.623 (0.0388)	7.8 (0.8060)	5.3 (0.3645)
Salix caprea	120551	-7.8555	1.4519	0.0317	0.624 (0.0074)	6.2 (0.1162)	3.3 (0.0396)

Table S3. Species-specific and broadleaves and conifers general allometric equations to estimate the total AGB and foliage biomass fraction according to pan-European models provided by Forrester et al. (2017b).

Species	Foliage biomass						Total AGB					
	β_0	β_1	N	R^2	RMSE	MAPE	β_0	β_1	N	R^2	RMSE	MAPE
Castanea sativa	−6.295 (0.287)	2.395 (0.057)	132	0.894	0.37	25.80	−1.835 (0.086)	2.291 (0.015)	297	0.974	0.15	9.46
Fagus sylvatica	−4.481 (0.162)	1.907 (0.019)	330	0.883	0.20	15.16	−1.659 (0.088)	2.358 (0.013)	330	0.981	0.16	9.35
Picea abies	−2.795 (0.085)	1.868 (0.016)	1007	0.906	0.26	17.63	−1.886 (0.052)	2.303 (0.011)	576	0.985	0.13	10.46
Pinus nigra	−0.610 (0.121)	0.870 (0.041)	66	0.871	0.10	8.03	−2.023 (0.139)	2.334 (0.028)	137	0.956	0.17	12.0
Pinus sylvestris	−3.527 (0.118)	1.747 (0.017)	848	0.858	0.27	20.37	−2.157 (0.077)	2.309 (0.014)	495	0.976	0.16	16.69
Prunus avium*	−4.105 (0.686)	1.321 (0.020)	99	0.545	0.15	10.99	-	-	-	-	-	-
Quercus ilex	−4.499 (0.219)	2.101 (0.050)	144	0.840	0.26	19.04	−1.741 (0.091)	2.369 (0.018)	210	0.987	0.14	8.47
Quercus robur	−4.466 (0.223)	2.137 (0.030)	99	0.910	0.16	12.14	−2.684 (0.414)	2.727 (0.025)	66	0.919	0.10	7.61
Broadleaves spp.**	−4.228 (0.099)	1.862 (0.013)	1824	0.846	0.36	27.92	−1.995 (0.043)	2.362 (0.006)	2223	0.978	0.18	11.15
Conifers spp.**	−3.401 (0.060)	1.907 (0.009)	3910	0.830	0.30	20.96	−2.208 (0.031)	2.378 (0.004)	2635	0.975	0.13	9.32

*The species Prunus avium count with allometric equations at genus level and the equations were for foliage, branches, and stem biomass, but a specific equation for the total AGB was obtained through the sum of the tree components. In order to simplify the table, only equations for foliage and AGB were shown, but all the equations at tree component levels are available in Forrester et al. (2017).
** Applied to all conifer and broadleaved species without specific allometric equations
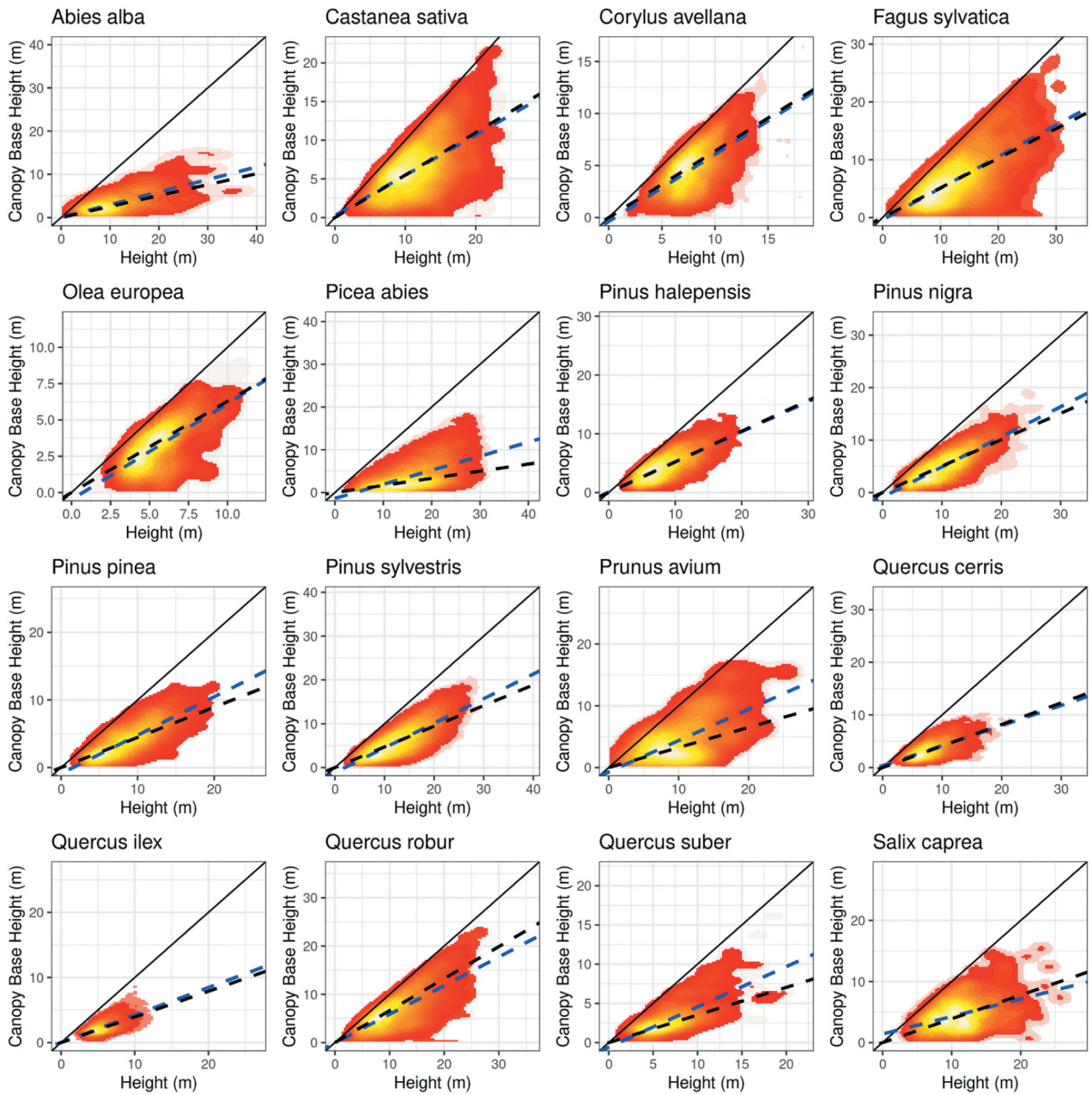
Figure S1. Fitted models for CBH estimation for the 16 species (see Table S1 for more details).
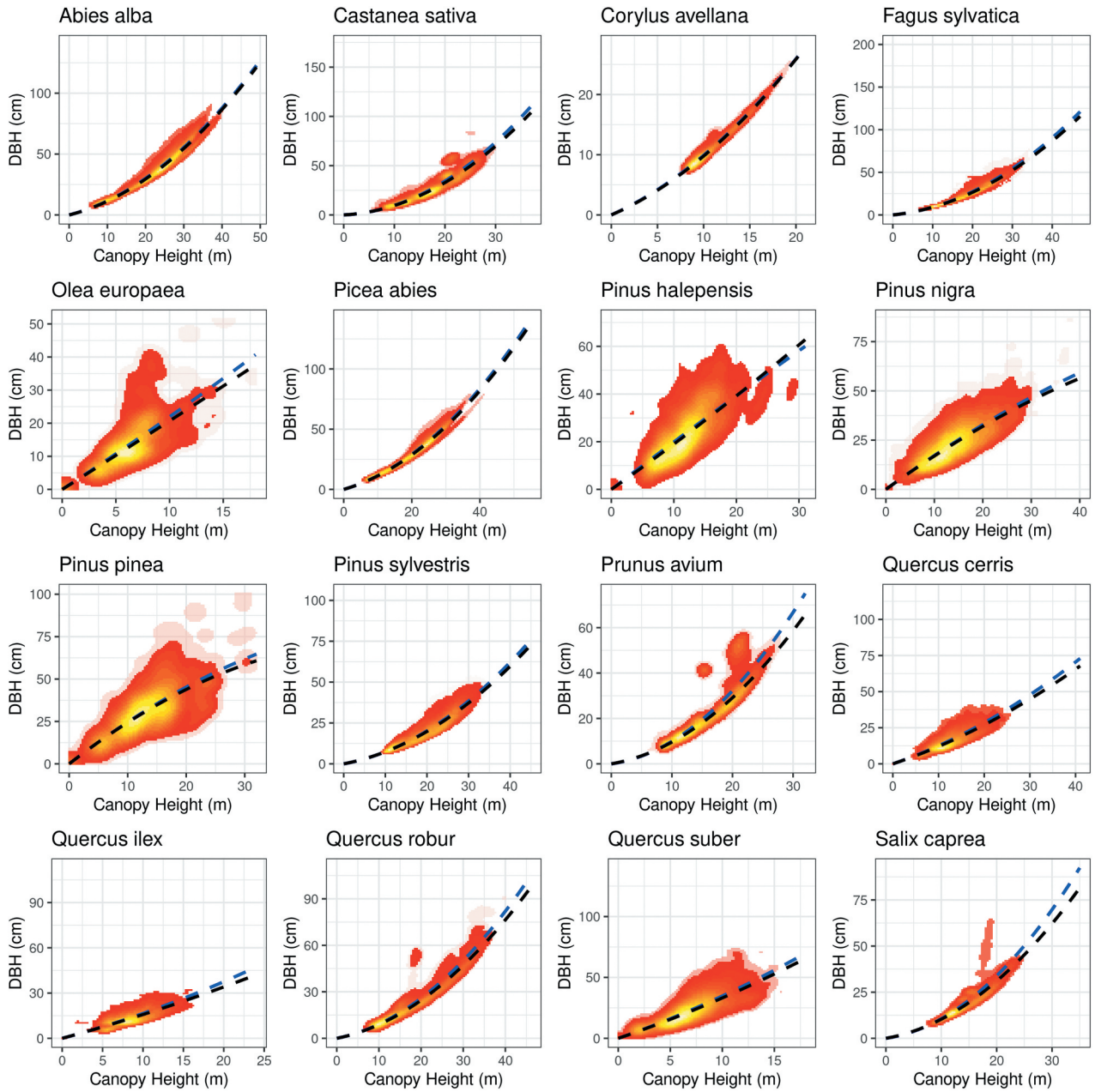
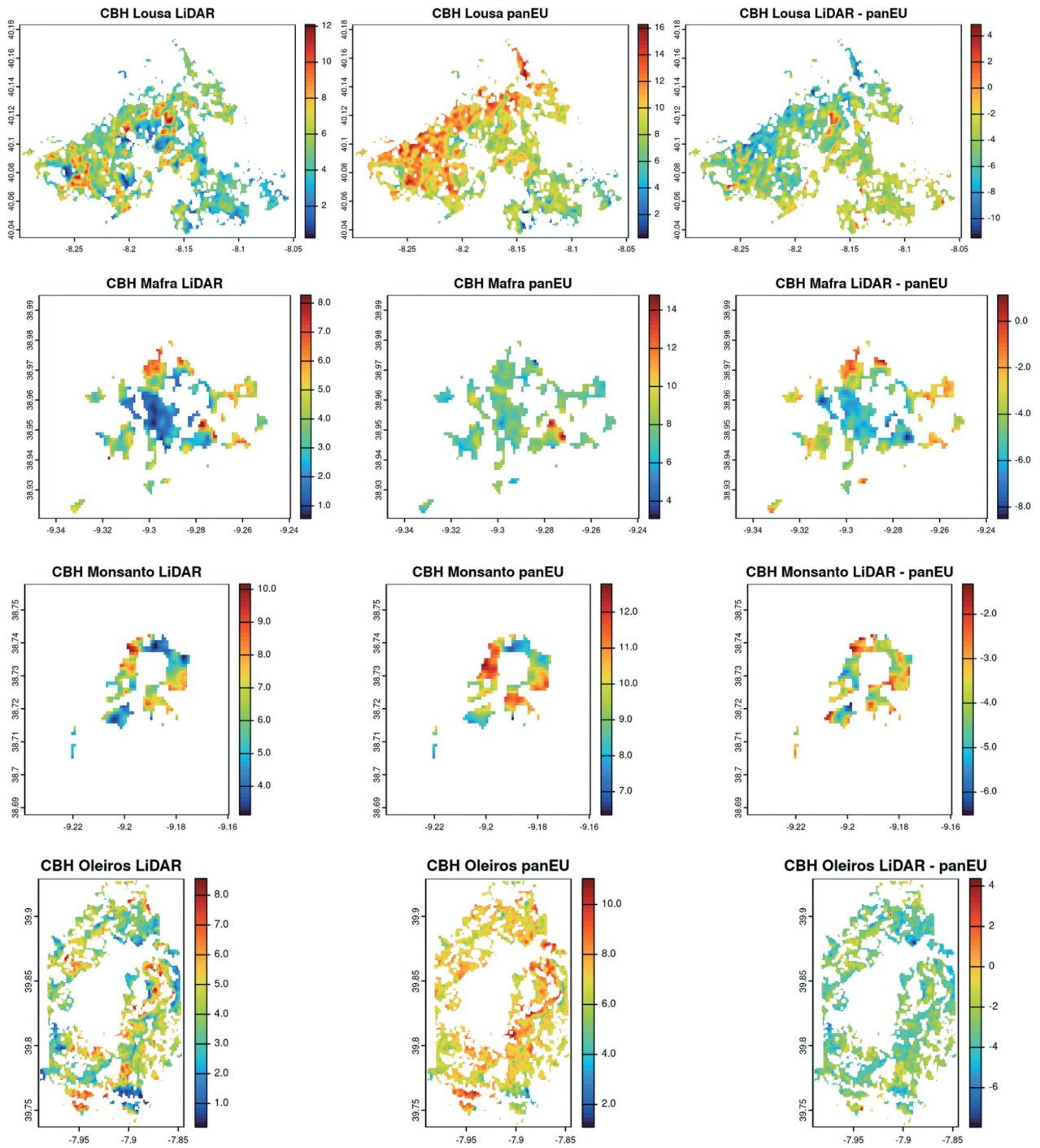**Figure S2.** Fitted models for DBH estimation for the 16 species (see Table S2 for more details).

Figure S3. Fitted models for CBH estimation for the 16 species (see Table S1 for more details).
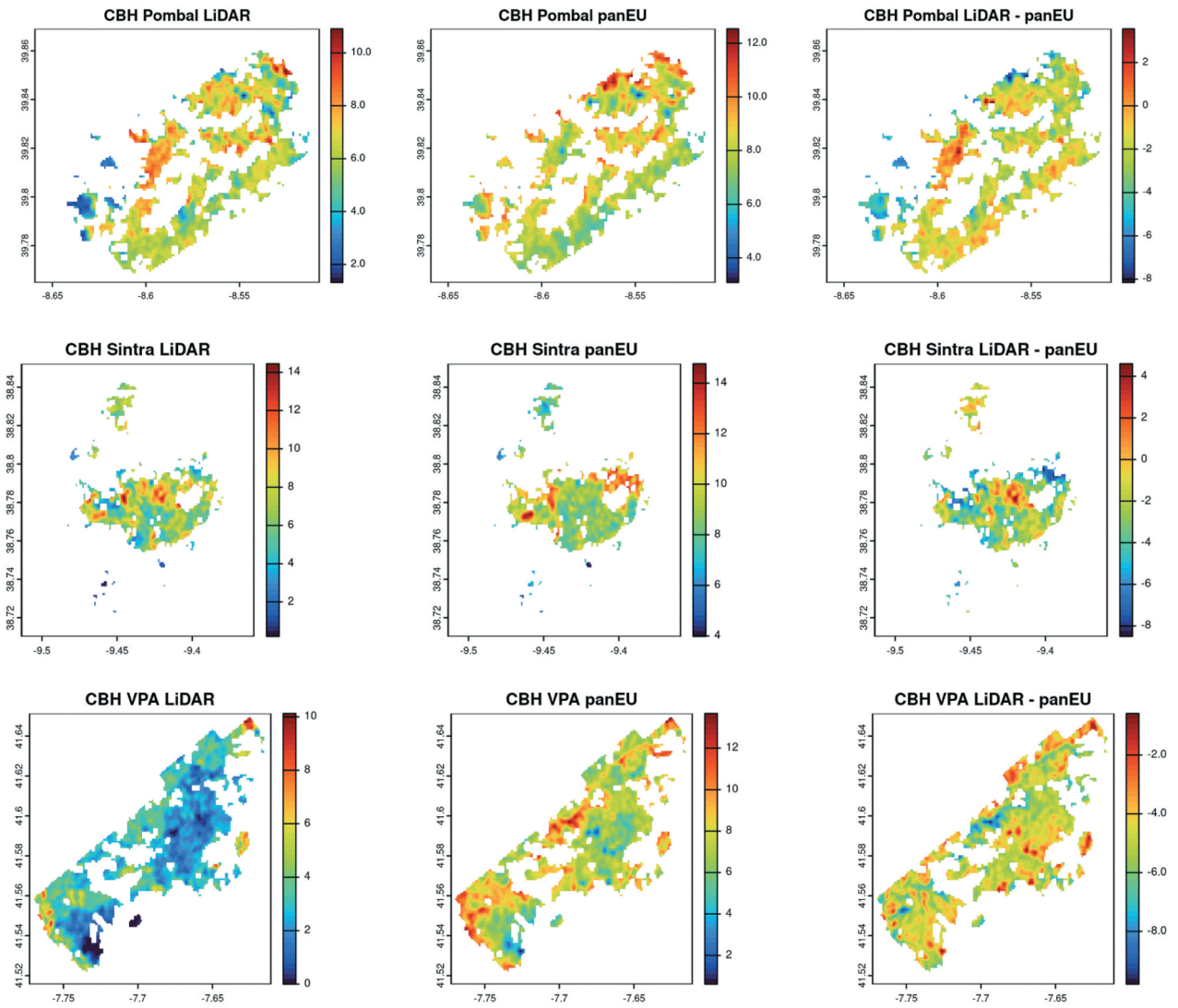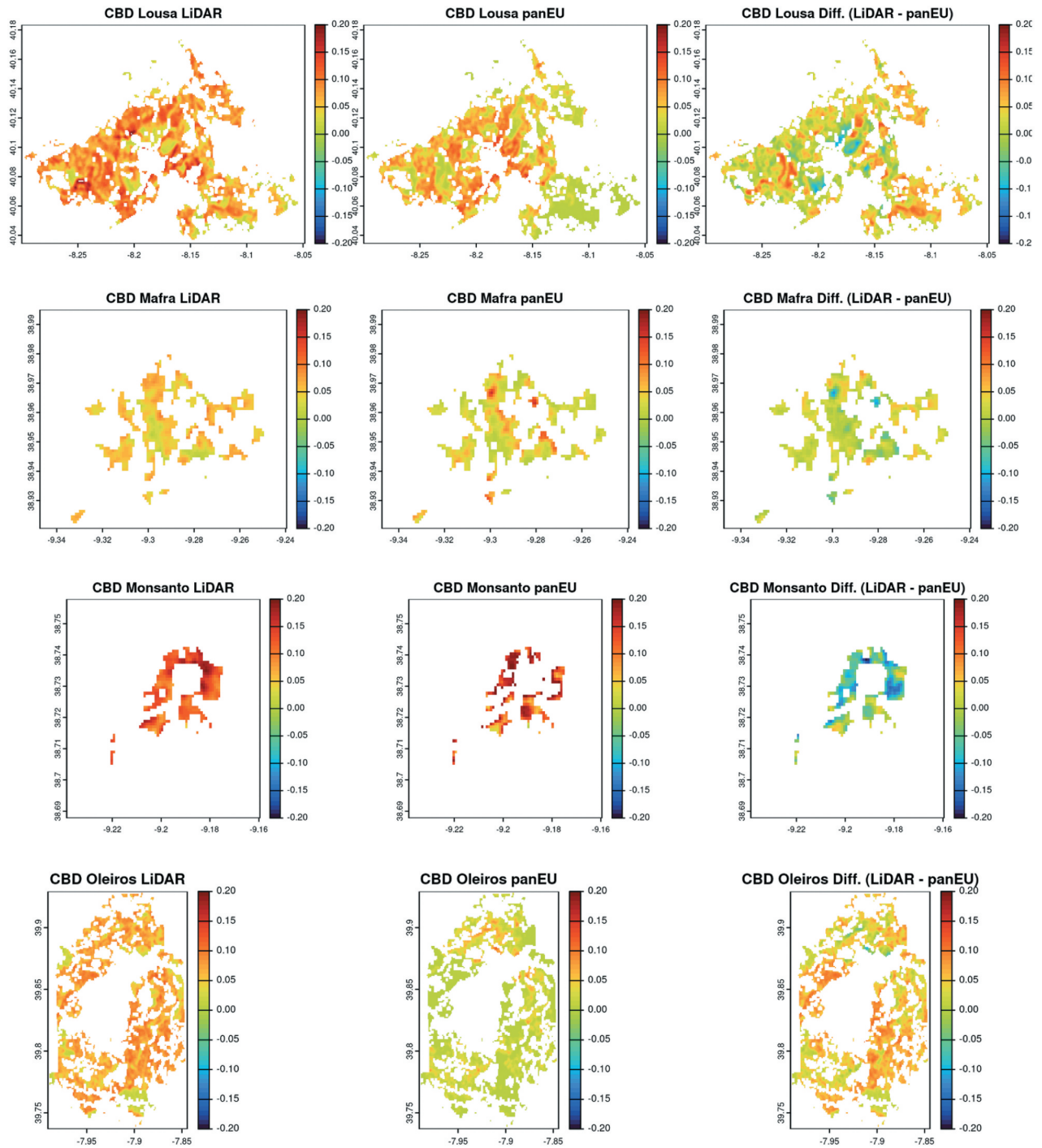
Figure S3. (Continued)

Figure S4. Areas with CBD extracted from LiDAR metrics (left) and from allometric models (center), with difference maps (right).
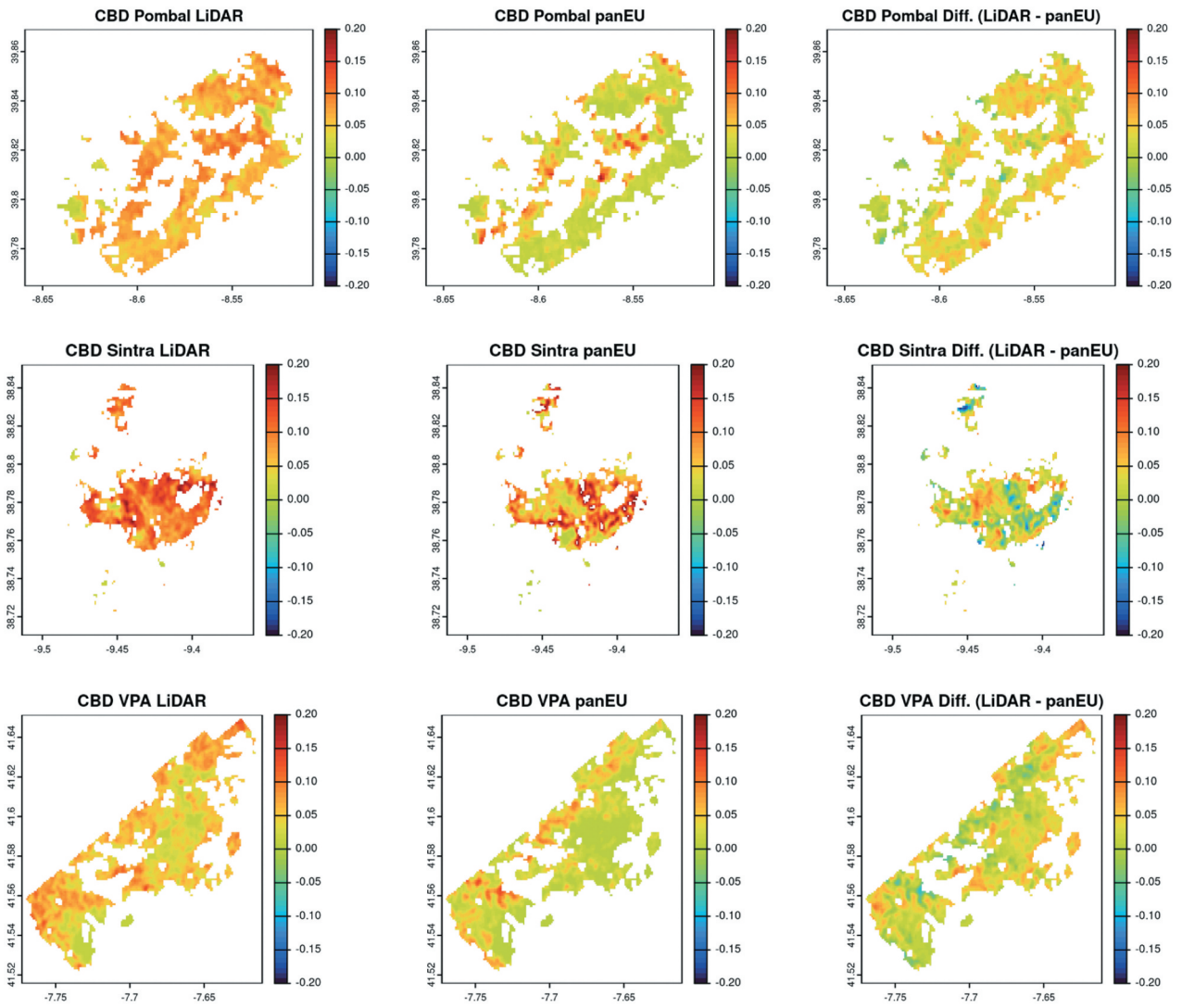
Figure S4. (Continued)